



Genetic rescue of Florida panthers reduced homozygosity but did not swamp ancestral genotypes

Diana Aguilar-Gómez^{a,b,1} , Lin Yuan^c , Yulin Zhang^b, Alexander Ochoa^d, Melanie Culver^{e,f}, Robert R. Fitak^g , Dave Onorato^h , Kirk E. Lohmueller^{a,i,1} , and Rasmus Nielsen^{b,1}

Affiliations are included on p. 11.

Edited by Anne Yoder, Duke University, Durham, NC; received June 28, 2024; accepted February 7, 2025

Pumas (*Puma concolor*) occupy a vast geographical range spanning from Canada to Argentina. Due to urbanization and unregulated hunting, pumas in Florida, known as panthers, are the only breeding population east of the Mississippi River. In the 1990s, Florida panthers numbered <30 individuals suffering from inbreeding depression. In 1995, eight pumas from Texas were translocated into southern Florida to mitigate the effects of isolation. This translocation reduced inbreeding depression and increased population size. While genetic rescue is often suggested as a means of ameliorating the effects of small population size, the underlying genetic mechanism and its long-term efficacy remain understudied. We sequenced the genomes of posttranslocation Florida panthers (PTFPs) to elucidate the genomic consequences of genetic rescue. We inferred local ancestry across the genomes of PTFPs and found that no regions have been entirely replaced by Texas ancestry, discarding the possibility of genetic swamping. Furthermore, the beneficial effects of the translocation were likely caused by a reduction in homozygosity, alleviating recessive deleterious load, rather than by a reduction in the number of deleterious variants. We did not find evidence that selection has favored replacement of original Florida DNA with Texas DNA in any systematic fashion. Using simulations, we found that heterozygosity increased in the long-term compared to a no translocation scenario; however, the effects on fitness are more transient. Our findings hold significant implications not only for the management of Florida's panther population, but also for informing strategies for genetic rescue in other wild, inbred populations encompassing broader conservation efforts.

genetic rescue | puma | conservation genomics | genetic swamping | florida panthers

Pumas (*Puma concolor*) are large carnivores that are distributed across a vast range stretching from the Canadian Province of British Columbia to the Chilean Strait of Magellan (1). Despite the extensive geographic distribution of pumas across the Americas, the subspecies of pumas in Florida (*P. concolor coryi*) (hereafter Florida panthers) remain the only viable population of pumas east of the Mississippi River, United States. The decline of panthers was primarily driven by unregulated hunting and fragmentation of habitat due to wide-scale urbanization in the region (2). By the early 1990s, Florida panthers existed as a small, isolated population of <30 individuals inhabiting Big Cypress National Preserve, Everglades National Park, and surrounding hardwood swamps and prairies in southern Florida (3). During this time, panthers confined to the Everglades displayed a mixture of native (i.e., canonical) and Central American (Panama-Costa Rica) ancestries resulting from poorly documented releases of captive-bred pumas in the area between 1956 and 1966 (4–9). In general, however, due to accrued effects of genetic drift and inbreeding, Florida panthers presented a depauperate canonical genetic variation and a high rate of developmental (e.g., atrial septal defects, kinked tails), reproductive (e.g., cryptorchidism, spermatozoal defects), and immunological (i.e., susceptibility to different biological agents) impairments (5, 10). Given these factors, population viability analyses projected the extinction of Florida panthers within 25 to 40 y absent immigration from other puma populations (11).

In 1995, eight female pumas from Texas were translocated into southern Florida as part of a genetic rescue plan to alleviate the occurrence of traits associated with inbreeding depression that would hopefully lead to an increase in abundance of the panther population (2, 12). In subsequent generations, five of these Texas pumas were documented to have produced at least 20 admixed Florida panthers, which collectively manifested an enhanced fitness relative to prerescue Florida panthers (13). For instance, van de Kerk et al. (14) found a positive correlation between kitten survival and their degree of Texas ancestry; a similar trend was noted for survival among adult and subadult age classes in Florida

Significance

In the mid 1990s, Florida panthers were at risk of extinction due to isolation and habitat loss with the population numbering less than 30 individuals, many of whom exhibited morphologic and genetic correlates of inbreeding. In 1995, eight female pumas from Texas were translocated to Florida to attempt "genetic rescue." We show that the rescue was successful with observed improvements due to increased heterozygosity rather than reduction in the number of deleterious variants. Further, our analysis shows that the Florida genetic ancestry was not completely replaced, thus allaying fears that rescue leads to extinction by replacement. We demonstrate that knowledge gained from speciation science can be applied to conservation action via the mechanism of genetic rescue from appropriately diverged populations.

The authors declare no competing interest.

This article is a PNAS Direct Submission.

Copyright © 2025 the Author(s). Published by PNAS. This open access article is distributed under [Creative Commons Attribution License 4.0 \(CC BY\)](#).

PNAS policy is to publish maps as provided by the authors.

¹To whom correspondence may be addressed. Email: aguilargomez@ucla.edu, klohmueler@ucla.edu, or rasmus_nielsen@berkeley.edu.

This article contains supporting information online at <https://www.pnas.org/lookup/suppl/doi:10.1073/pnas.2410945122/-DCSupplemental>.

Published July 28, 2025.

panthers. Moreover, at the genomic level, F₁ panthers exhibited a nearly threefold increase in observed heterozygosity with respect to the previous, canonical Florida generation (7, 15). This genetic rescue project also had positive long-term effects on Florida panther fitness, as exemplified by the declines in proportion of individuals examined that exhibited cryptorchidism, atrial septal defects, and abnormal sperm when comparing cohorts of panthers born prior to genetic rescue versus admixed panthers born post-genetic rescue (16). As of 2023, the Florida panther population size is believed to range between 120 and 230 adults and sub-adults (17).

The benefits of translocating individuals with the intent of genetic rescue have, at times, been controversial (18–20). One potential benefit is the introduction of new genetic variation into populations affected by accumulation of (primarily additive) deleterious variants due to reduced population size. If a substantial number of deleterious variants have gone to fixation during a bottleneck, introducing new chromosomes that do not carry these variants can serve as a substrate for selection removing deleterious variants. This in turn may provide substantial gains in fitness after recovery from a bottleneck (21). Another potential benefit is the masking of recessive deleterious alleles due to increased heterozygosity after genetic rescue (22). This effect does not require selection to act, will be effective immediately after genetic rescue, even in the absence of a population size recovery, but requires that a substantial proportion of the original population is replaced by the donor population (23, 24). Hitherto, the exact genomic mechanism causing an increase in fitness after genetic rescue remains unknown.

Potential drawbacks of genetic rescue include the possibility of genomic swamping, i.e., the replacement of the local DNA by DNA from the donor population that may eliminate local adaptive genetic variation (13, 25, 26). This will be a particular risk in systems where individuals from the donor population carry substantially fewer deleterious alleles so that selection will strongly favor the donor population chromosomes (23, 24, 27). Another potential drawback is the possibility the donor population will introduce new deleterious variants (19, 20). If the rescued population has had a small population size for a long period of time, it may have purged recessive deleterious variants, and the introduction of new genetic variation might actually have an overall detrimental effect. In the case of Florida panthers, this is likely not an issue since it is well documented that the population decline was associated with recent human activity (2). However, Ochoa et al. (15) described an increase in the number of heterozygotes carrying deleterious alleles in the F1 generation compared to the pretranslocation Florida panthers. Epistatic interactions between alleles from the donor and the rescued populations may also lead to reductions in fitness (28). While it is clear that the genetic rescue in Florida panthers increased fitness, the degree that it may also have caused genetic swamping is unclear. In this study, our goal is to understand the genomic effects of the genetic rescue on heterozygosity and deleterious variation and determine whether genetic swamping occurred.

Results

Genetic Structure of Puma Populations. To assess the genomic consequences of genetic rescue via translocation, we generated whole genome sequence data from 29 posttranslocation Florida panthers (PTFPs) (29) (Fig. 1B; also see *Materials and Methods* and [Dataset S1](#)). To contextualize our findings within the species, we combined these data with publicly available whole-genome

sequence data from two previous studies (7, 8) (Fig. 1A). We included two individuals from Brazil (BR); five individuals from California, including three from the Santa Monica Mountains (SMM) and two from Santa Cruz (SC); and one from Yellowstone (YNP). Texas (TX) samples comprise the five individuals who were introduced in Florida for genetic rescue in 1995 and successfully mated. We also included two samples from Everglades (EVG) panthers with mixed ancestry (previously noted) and four canonical Florida panthers (CFP). In addition to our 29 PTFP samples, we included two F₁ (CFPxTX) PTFP individuals (7).

We mapped all reads to the reference genome of *Puma yagouaroundi*, and after filtering and applying a 5% minor allele frequency filter (*Materials and Methods*), we performed Principal Component Analysis on the genetic data (Fig. 1C) to assess patterns of population structure. PC1 separates North and South American populations, with EVG clustering in the center, consistent with the known introduction of captive pumas from Central America in that area (4–9). PC2 separates pumas across North America from West to East, with California at the left, followed by Yellowstone, Texas, and Florida at the right. The PTFP samples fall between CFP and TX, as expected.

To further explore genetic structure, we used OHANA (31) to estimate the admixture proportions assuming a standard admixture model in each individual, specifying different numbers of ancestry components (k), while using genotype likelihoods to take uncertainty in genotyping into account. Specifying k = 3, we obtained one component for Central and South America, and two components for North America, separating the populations in West (California) and East (Florida) and some populations being a mix of Eastern and Western ancestral puma components (Texas and Yellowstone) (Fig. 1D). When k = 4, California and Texas separate and each are assigned their own component.

Heterozygosity and Inbreeding After Translocation. We analyzed genetic relatedness among the pumas using ngsRelate (32), which uses genotype likelihoods and accounts for inbreeding within a population. Before the translocation, CFPs had inferred relatedness values ranging between 0.44 and 0.72, with an average of 0.57, which is similar to the level of relatedness expected for siblings or parent–offspring in outbred populations (Fig. 2A and [Dataset S2](#)). After the translocation, the relatedness of PTFP individuals decreased to an average of 0.03 (min = 0, max = 0.56).

We calculated heterozygosity in sliding windows across the genome (size = 100 kb, step = 10 kb). The CFPs and Santa Monica Mountains (SMM) pumas have more genomic regions with zero heterozygosity than other groups we sampled (Fig. 2B). We next searched for ROHs of different lengths (short 0.1 to 1 Mb, medium 1 to 10 Mb, and long >10 Mb) in each genome and calculated the fraction of the genome in ROHs (>1 Mb; Fig. 2C). We found that CFP individuals have the greatest number of long ROHs (30% of their genome is in ROHs >10 Mb). In contrast, Texas (TX) individuals have on average 2% of their genome in long ROHs. The main reason that TX individuals were chosen to be introduced into Florida in 1995, was the historical gene flow suspected between these populations (2) and the lack of morphological defects in TX, which seemed to indicate a genetically healthy population (12). At the time, genomic technologies were not available. Genomic sequencing confirmed that TX and Yellowstone (YNP) have the highest heterozygosity among the North America samples included in this study ($\pi_{TX} = 0.00089$, $\pi_{YNP} = 0.00093$), excluding Everglades (EVG), which will be discussed below. Second only to individuals from Brazil (BR), TX individuals have the lowest fraction of their genome in ROHs

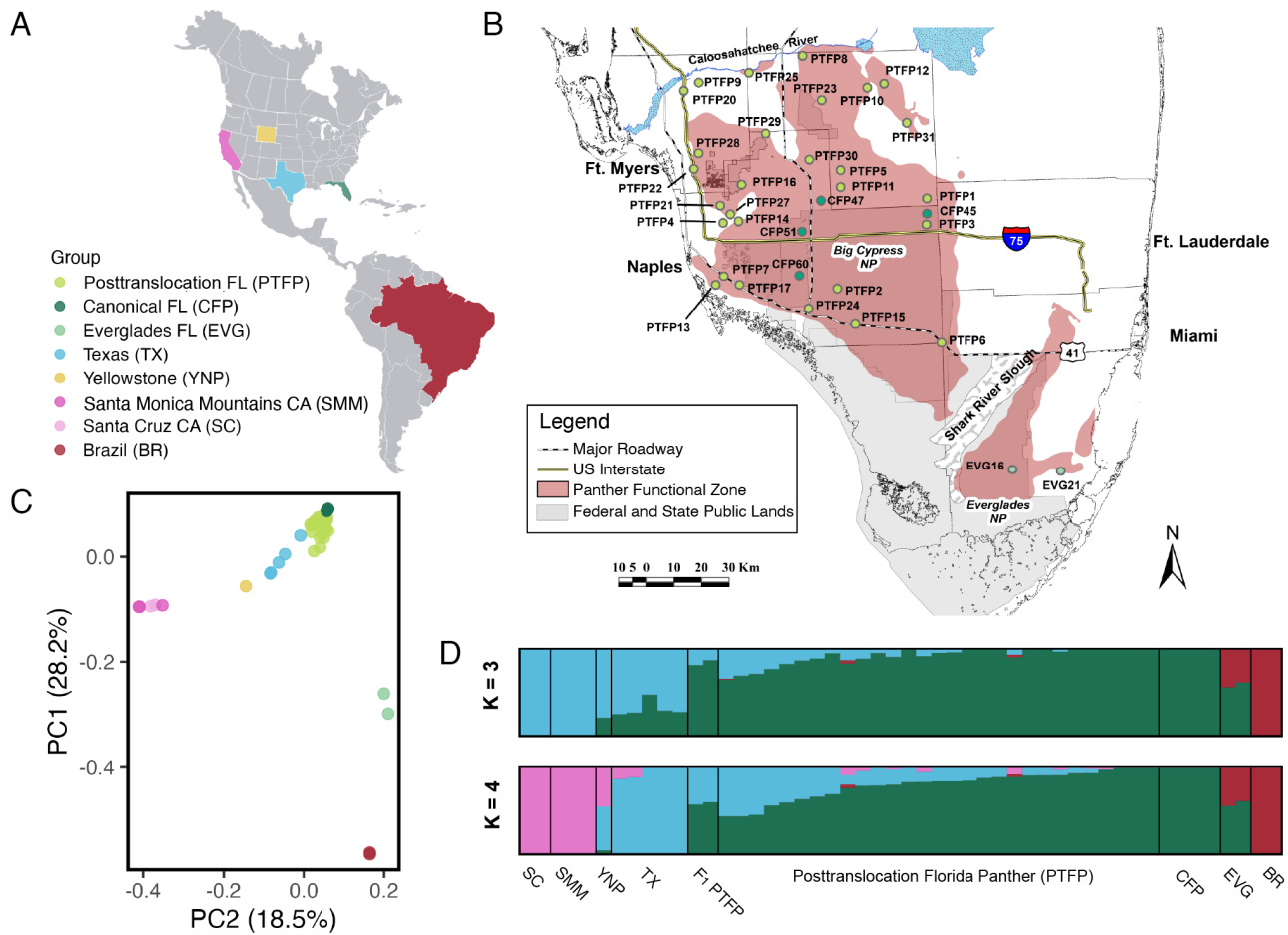


Fig. 1. Sampling locations and population structure of pumas in the Americas. (A) Map of the sampling regions and code used for the different groups analyzed. (B) Collection locations for Florida panther (*P. concolor cory*) samples in South Florida, USA. The Panther Functional Zone comprises suitable habitat that supports the breeding population of panthers in South Florida from the Caloosahatchee River south to Everglades National Park (30). Three PTFPs are not shown in this map, as they were collected north of this zone. (C) Principal component analysis of puma SNPs with a 5% minor allele frequency filter. (D) OHANA unsupervised ancestry component analysis, specifying $K = 3, 4$.

(Fig. 2D), with most of it in small ROHs (Fig. 2C). Individuals from BR are the least inbred, having the highest heterozygosity (0.00178) and only 5% of their genome in ROHs. The average heterozygosity in EVG pumas (0.00117) is more than three times greater than that in CFP pumas (0.00031). However, EVG pumas have a large proportion of long ROHs (19% of their genome in ROHs >10 Mb) and more than 35% of their genome in ROHs (Fig. 2D). In the case of the PTFPs, heterozygosity increased (to 0.00073) on average more than 2 \times what it was before genetic rescue. The average fraction of the genome in ROHs was reduced to less than half the levels pregenetic rescue (CFP = 63%, PTFP = 28%) (Fig. 2D), particularly reducing long ROHs (CFP = 30%, PTFP = 11%) (Fig. 2C). Our results (Fig. 2D) match the findings of Saremi et al. (8), but we expand those results to include individuals from Texas, posttranslocation Florida, and additional individuals from California, Everglades, and canonical Florida absent from that study.

Preservation of Local Ancestry and Heterozygosity. To evaluate local ancestry along the genomes of PTFPs, we used ancestryHMM (33) to identify regions of original Texas (TX) and Florida (FL) ancestry. In contrast to the ancestry component analysis using OHANA (Fig. 1D), ancestryHMM infers all PTFP to be admixed, with 24 to 61% TX ancestry (*SI Appendix, Table S1*). Within each individual, we compared genomic ancestry (*Materials and Methods*) to heterozygosity in sliding windows (size = 100 kb, step

= 10 kb). We found that the regions that are homozygous for FL ancestry are almost completely depleted of heterozygosity, and reside in long ROHs (Fig. 3A and B). Within PTFP individuals, the distribution of heterozygosity in windows with homozygous FL ancestry (Fig. 3B) looks similar to that of CFPs (Fig. 2B).

We did not find any regions in our genomic sequences (confidence inferences with posterior probability $>95\%$) where the local ancestry inferences of PTFP individuals were completely replaced by Texas ancestry, which would be indicative of genetic swamping (Fig. 3C). This demonstrates that local alleles are being retained in the Florida population post-genetic-rescue.

Simulated Effects of Genetic Rescue on Heterozygosity and Fitness Detected. We used SLiM simulations (34) to predict how ancient demographic history and genetic rescue affects heterozygosity and fitness (35). We obtained effective population sizes (N_e) and divergence parameters from a previous study that used $\partial\alpha/\partial t$ to infer the demography taking into account inbreeding (36). We simulated the following scenarios: A) genetic rescue of CFPs by introduction of pumas from Texas (TX), and B) the same demographic model as A without any gene-flow (Fig. 4A and B). In both scenarios, the simulated CFP population experienced a severe bottleneck ($N_{e,CFP2} = 7$) and then recovered to a very small population size ($N_{e,CFP3} = 50$). Scenario B serves as a baseline to evaluate how population size alone affects genetic variation and fitness, allowing us to assess the effects of the rescue. We simulated

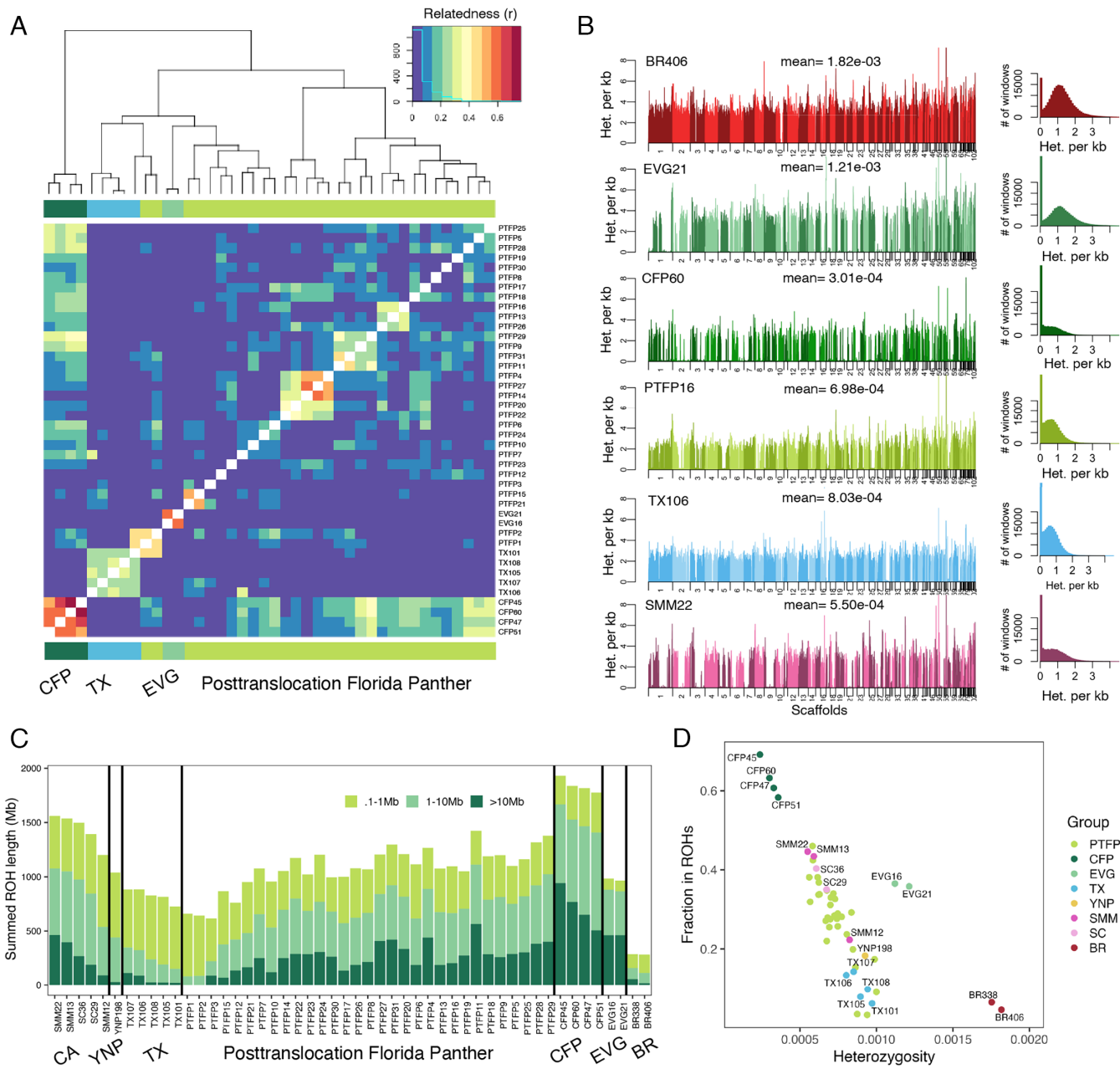


Fig. 2. Relatedness, heterozygosity, and ROHs. (A) Relatedness matrix of populations in Florida and Texas. (B) Each row shows on the left the genome-wide heterozygosity of one representative individual per population (window size = 100 Kb, step = 10 Kb) and on the right a histogram of the distribution of heterozygosity across windows. From top to bottom, the individuals are Brazil (BR406), Everglades (EVG21), canonical Florida panther (CFP60), posttranslocation Florida panther (PTFP16), Texas (TX106), and Santa Monica Mountains (SMM22). Each plot is labeled with the sample name and the mean genome-wide heterozygosity. (C) Distribution of runs of homozygosity (ROHs) in each individual, divided into three bins: short 0.1 to 1 Mb, medium 1 to 10 Mb, and long >10 Mb. Vertical panels separate by region: California (CA), Yellowstone (YNP), Texas (TX), posttranslocation Florida panther (PTFP), canonical Florida panther (CFP), Everglades (EVG), Brazil (BR). (D) Scatter plot of the fraction of the genome in ROHs (>1 Mb) vs. heterozygosity per individual.

both scenarios under a partially recessive model dominance effect ($b = 0.45$, $s > -0.001$), ($b = 0.2$, $-0.001 \geq s > -0.01$), ($b = 0.05$, $-0.01 \geq s > -0.1$), ($b = 0.0$, $s \leq -0.1$) (37) and a model with only additive effects ($b = 0.5$).

Considering heterozygosity, one generation prior to the severe bottleneck, heterozygosity is only slightly lower in the simulated CFP compared to the simulated TX population due to the different ancestral population sizes ($N_{e_{TX}} = 31,150$, $N_{e_{CFP1}} = 704$) (Fig. 4 C and D). The bottleneck has a similar impact on heterozygosity for both dominance models, (Fig. 4 and *SI Appendix*, Fig. S1A). At this time, the simulated CFP population has fairly uniform levels of heterozygosity across the genome with an average of 0.00005 per bp. During the bottleneck ($N_{e_{CFP2}} = 7$), heterozygosity decreases in

certain segments of the genome, while remaining high in others (Fig. 4D). For both dominance models, the heterozygosity increases five generations after translocation by an order of magnitude (Fig. 4E and *SI Appendix*, Fig. S1A), to levels higher than those observed before the bottleneck. Further, gene flow reduced the number of segments of the genome with very low heterozygosity, resulting in a more pronounced bimodal distribution (Fig. 4E). Here, the patterns of heterozygosity in the simulated CFP genomes qualitatively mimic those of the empirical data (compare Fig. 4 D and E to Fig. 2B), suggesting that translocation is a plausible mechanism which led to the genome-wide patterns. Note that simulations without the translocation show low heterozygosity across the genome, and a unimodal distribution of heterozygosity (Fig. 4F), inconsistent

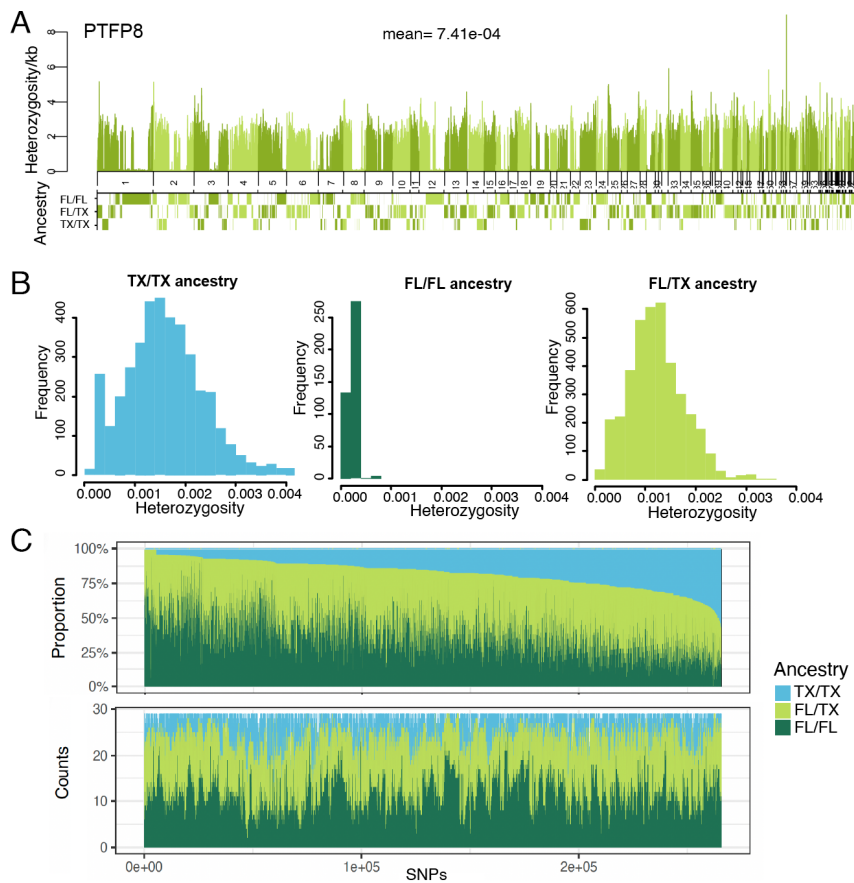


Fig. 3. Local ancestry and heterozygosity. (A) Genome-wide heterozygosity per kb of a posttranslocation FL panther and the inferred ancestry aligned by scaffold. The plot is labeled with the sample name and the mean genome-wide heterozygosity for that individual. (B) Histogram of heterozygosity of windows that correspond to each of the inferred ancestries in the same individual (PTFP8). TX: Texas, FL: Florida. (C) Top: sorted proportion of individuals that have each of the ancestry inferences. Bottom: counts of individuals with each ancestry. SNPs are sorted by position in the scaffold. F_1 samples were excluded from these plots because they are FL/TX everywhere.

with the empirical data (Fig. 2B). As time since the bottleneck increases, heterozygosity decays in both scenarios.

Considering fitness, immediately after the bottleneck, there is a reduction in fitness in CFP in the model involving partially recessive effects (Fig. 5 A and B), but not in the model with only additive effects (Fig. 5 C and D) suggesting a higher load due to partially recessive deleterious variants being exposed in the homozygous state in CFP (*SI Appendix*, Table S3). On average, in all models, the translocation scenario resulted in genetic rescue (increased fitness compared to the no translocation scenario). However, this increase in fitness is transient, as fitness drops again within 20 generations of gene flow (Fig. 5 A and B). In the model without translocation, fitness increases more slowly after the bottleneck, and about 100 generations after the bottleneck, the fitness after translocation is only slightly higher than that without the translocation (Fig. 5 A and B). The increase in fitness is transient because the population size remains small ($N_{e_{CFP3}} = 50$), increasing homozygosity for deleterious variants over time. Indeed, the slight long-term increase in fitness due to translocation is not seen consistently across all individual simulation replicates, suggesting that the long-term benefits of translocation are subject to chance (*SI Appendix*, Fig. S4). In the additive model, fitness is more stable over time, although it slowly decreases due to accumulation of deleterious variants (Fig. 5 C and D). In sum, our results suggest that the observed benefits of genetic rescue are likely due to increased heterozygosity dampening the effects of recessive deleterious variants that otherwise would be exposed in the homozygous state.

To account for the parameter uncertainty, we also implemented models with different demographic scenarios: one with a more recent split between CFP and TX and smaller ancestral population size before the bottleneck (Fig. 5 E and F); another with an older split time and larger ancestral population time (Fig. 5 G and H). In terms of the patterns of heterozygosity, both models have similar results to the original model (*SI Appendix*, Fig. S1). When considering fitness, both scenarios have a sharp increase in fitness after translocation, followed by a decline, mimicking the original model. This pattern is likely due to the initial alleviation of homozygosity by introducing new alleles; the drop is a consequence of introducing all types of alleles, including deleterious ones. The recent split model had a lower fitness before the translocation (*SI Appendix*, Table S3 and Fig. 5E) due to its smaller population size ($N_{e_{CFP1}} = 56$). Interestingly, the difference in fitness between the translocation and no translocation scenarios is the largest in this model. Perhaps the population with the lower starting fitness can be better rescued by translocation. Alternatively, it might suggest that translocation from a less diverged population is more effective in genetic rescue.

Deleterious variation in empirical puma genomes after genetic rescue. We assessed the patterns of putatively deleterious amino acid changing variants across the puma genome. To do this, we annotated variants that fell in coding regions using SIFT (38) to predict whether they are deleterious or tolerated. We found that when comparing the ratio of deleterious/tolerated alleles within individuals, Texas (TX) had a lower proportion of deleterious alleles

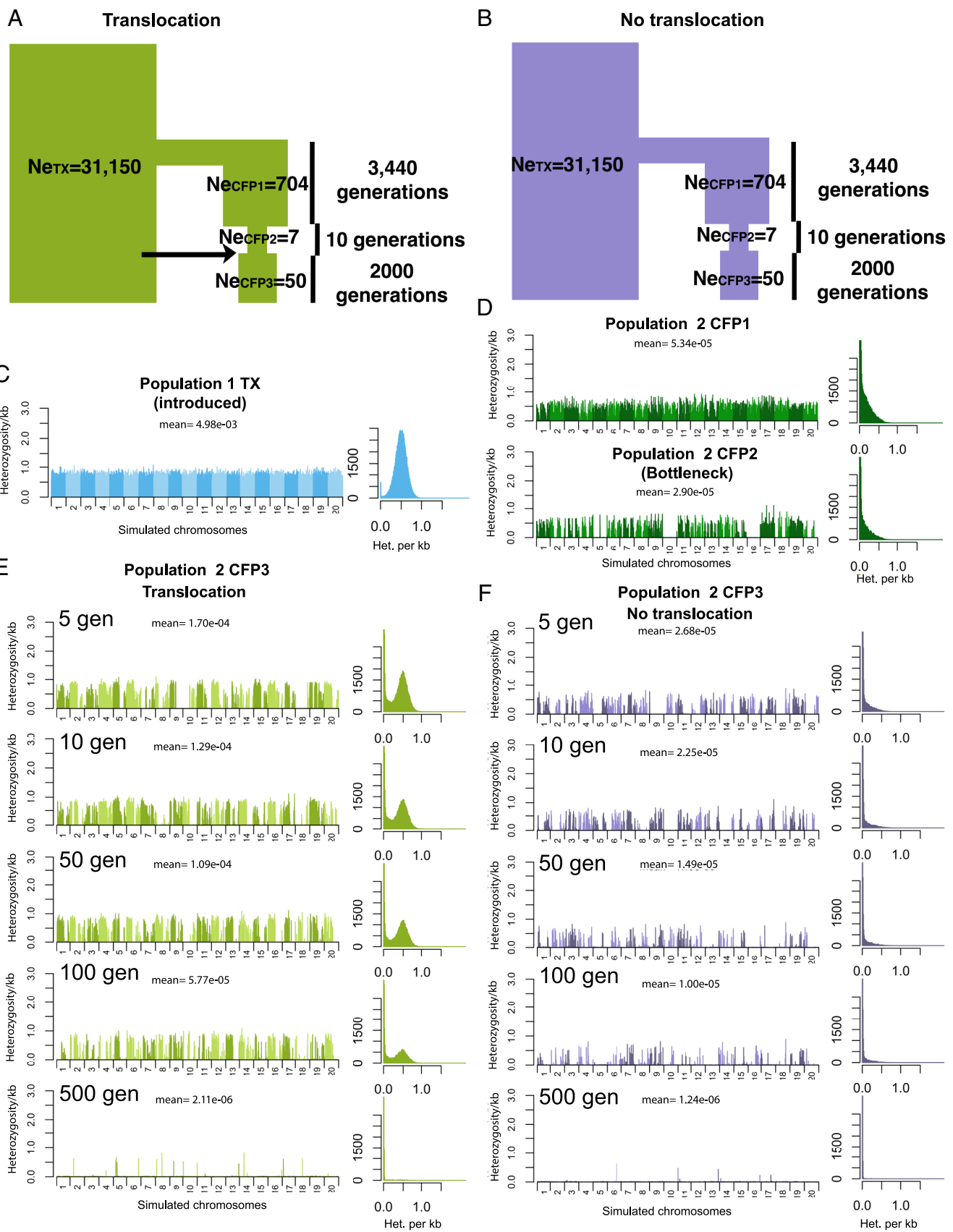


Fig. 4. Simulations of ancestral demography and translocations and their effect on genome-wide heterozygosity under a partially recessive model. (A) Model of CFP-TX with translocation. (B) Model of CFP-TX with no translocation. Panels C–F show a Manhattan plot of the genome-wide heterozygosity and a histogram of those values to the right. Each panel shows one representative individual from each population and is labeled with the mean genome-wide heterozygosity. (C) Simulated TX population. (D) Simulated CFP population, Top panel before severe bottleneck ($Ne_{CFP1} = 704$), Bottom panel during severe bottleneck ($Ne_{CFP2} = 7$). (E) Simulated CFP population X number of generations after translocation and population expansion ($Ne_{CFP3} = 50$). (F) Simulated CFP population after expansion.

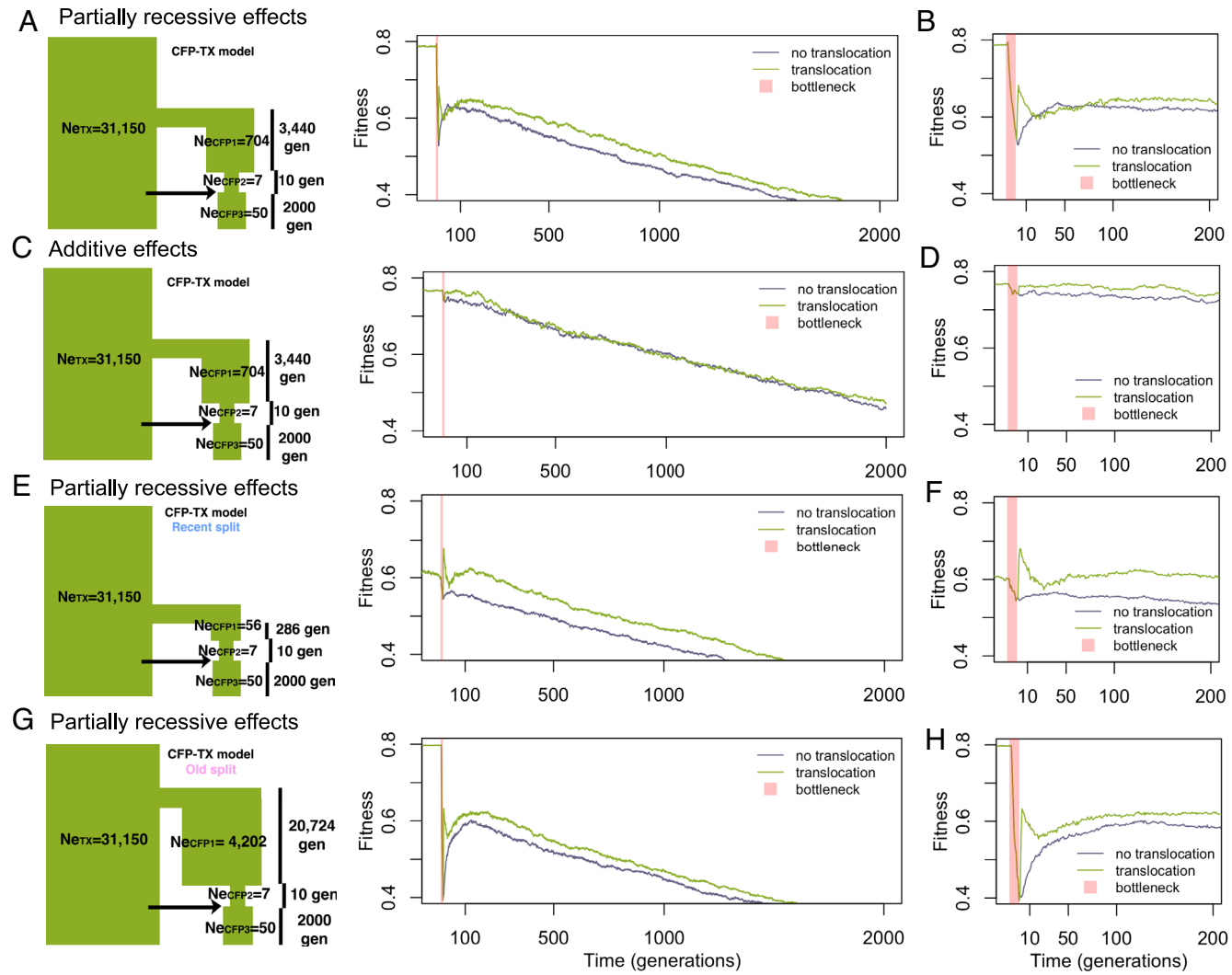


Fig. 5. Average fitness over time in simulations. Fitness is scaled relative to an individual with no deleterious variants. Models with translocation are in green and models with no translocation are purple. Left panels (A, C, E, and G) show the demographic model and a plot of the fitness starting before the severe bottleneck ($N_{e,CFP2}$) until 2,000 generations after the population expansion ($N_{e,CFP3}$). Right panels (B, D, F, and H) display the fitness in the first 200 generations after the bottleneck ($N_{e,CFP3}$). (A and B) Partially recessive model of the original model. (C and D) Additive effects model in the same model. (E and F) Partially recessive model with more recent split time between TX and CFP. (G and H) Partially recessive model with older split time between TX and CFP.

than CFPs, though this difference was slight and not statistically significant (Wilcoxon CFP-TX P -value = 0.1111, *SI Appendix*, Fig. S2A). The PTFPs had a slightly higher proportion of deleterious alleles than CFP, but this difference was also not significant (Wilcoxon CFP-PTFP P -value = 0.5649, *SI Appendix*, Fig. S2A). Taking into account only homozygous genotypes, TX had the lowest proportion of homozygous deleterious variation and the differences with the Florida populations were significant (Wilcoxon PTFP-TX: P -value = 0.00104 Wilcoxon CFP-TX: P -value = 0.01587, *SI Appendix*, Fig. S2B). After rescue, Florida panthers had a decreased proportion of homozygous deleterious variation compared to before genetic rescue (Wilcoxon CFP-PTFP P -value = 0.00069, *SI Appendix*, Fig. S2B). When we assessed the loss of function (LOF) variants annotated using snpEff (39, 40) there was an increase in the number of derived LOF alleles per individual after the rescue (Wilcoxon CFP-PTFP P -value = 0.005921, *SI Appendix*, Fig. S2D), but fewer homozygous LOF genotypes (Wilcoxon CFP-PTFP P -value = 0.01646, *SI Appendix*, Fig. S2E).

In PTFP individuals, we found a significant correlation between deleterious homozygous genotypes and the proportion of the genome with no TX ancestry ($R^2 = 0.65$, P -value = 6.2e-08). We also found a significant correlation between homozygous LOF

genotypes and the proportion of the genome with no TX ancestry ($R^2 = 0.41$, P -value = 0.00016). The individuals with less TX ancestry have more homozygous deleterious and LOF variants (*SI Appendix*, Fig. S2). However, we observed similar correlations between homozygous Florida ancestry and predicted tolerated variants ($R^2 = 0.37$, P -value = 0.00036, *SI Appendix*, Fig. S2J-L), suggesting that the decrease in homozygosity is a genome-wide phenomena driven by admixture.

Selection for Ancestry Postgenetic Rescue. While we found no evidence of genetic swamping (Fig. 3C), we were interested in the possibility of selection after rescue leading to an enrichment of ancestry depending on the local gene density in the genome. An increase in Texas (TX) ancestry in gene-rich regions would indicate that selection might be acting to increase TX ancestry in functionally important regions. We divided the genome into nonoverlapping windows of 5 Mb, calculated gene density and ancestry proportion in each window (*Materials and Methods*), and investigated the correlation between these two variables (Fig. 6A). We found that gene density and ancestry are not significantly correlated at this scale ($R^2 = 0.00021$, P -value = 0.7692). Thus, we do not find evidence that selection has favored replacement of

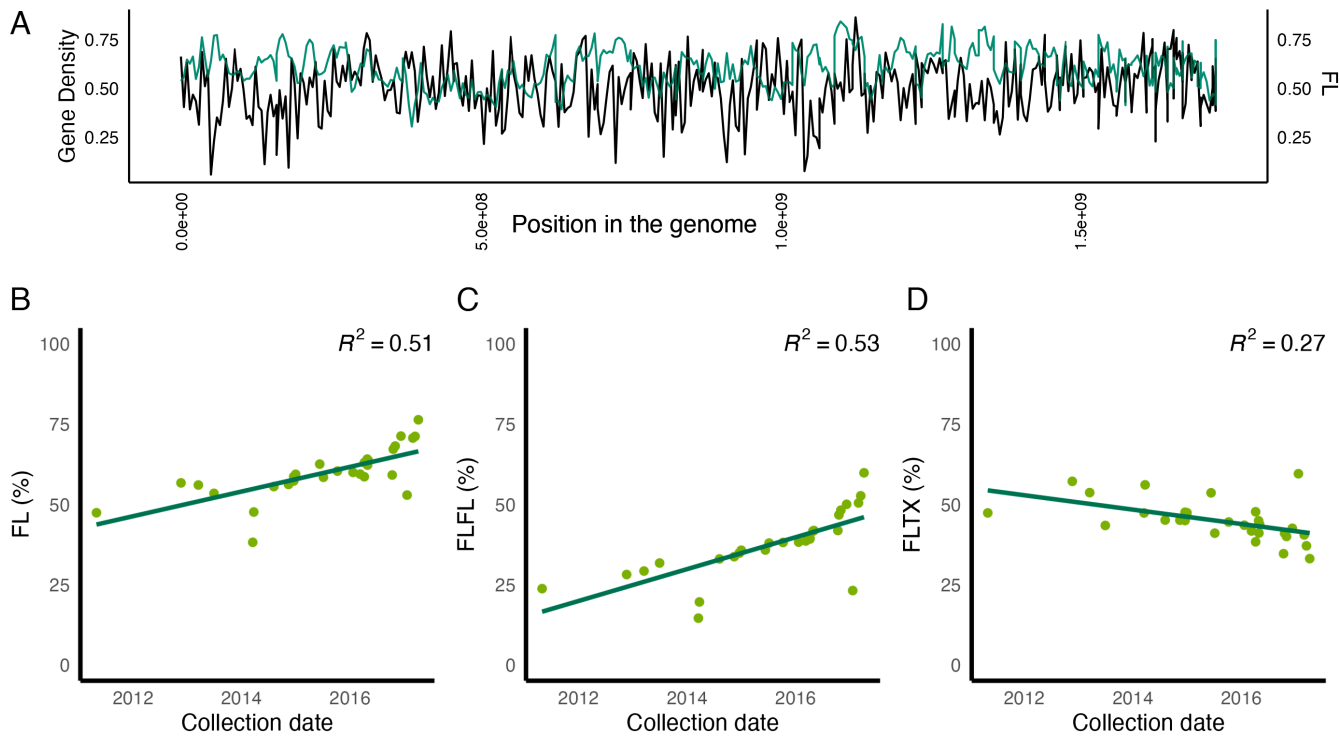


Fig. 6. Testing for natural selection after genetic rescue. (A) Gene density (proportion of a 100 Kb window that is covered by a gene) in black and proportion of individuals with Florida ancestry in each window in green. (B) Collection date of PTFPs and Florida ancestry (FL%). (C) Collection date of PTFP and homozygous Florida ancestry (FLFL%). (D) Collection date of PTFP and heterozygous ancestry (FLTX%).

original Florida DNA with Texas DNA in any systematic fashion. This further supports the hypothesis that the beneficial effect of genetic rescue is to increase heterozygosity, diminishing the effect of recessive deleterious alleles, rather than reducing the overall number of deleterious alleles.

To assess whether the proportions of Florida and Texas ancestry are shifting over time, we analyzed the correlation between collection date and ancestry proportions of PTFPs, excluding F1 individuals. Our results indicate an increase in Florida ancestry over time (Fig. 6). More recently collected panthers exhibit higher Florida ancestry (Fig. 6 B and C) and show fewer genomic regions with admixed ancestry (Fig. 6D). While this pattern could be explained by a number of factors (*Discussion*), we searched for signals of positive selection using several selection scan methods (*SI Appendix*, Fig. S3). However, we did not find any obvious signals of local selection.

Discussion

Here, we combined whole-genome sequence data with population genetic simulations to investigate the genomic impact of genetic rescue in Florida panthers. Overall, we found that the translocation had several beneficial effects including a reduction in homozygous genotypes for deleterious variants, an increase in genetic variation, a reduction of relatedness, and a reduction of ROHs. The long-term (>50 generations into the future) benefits of the translocation on population fitness and heterozygosity are less certain, however.

One of the major concerns when translocating individuals for genetic rescue is the potential for genetic swamping, where the original ancestry is completely replaced by ancestry from the migrant population (22, 24, 25). The genetic rescue of Florida panthers was necessitated by predictions that the population would become extinct within a century without some form of management

initiative (11). Translocation with the intent of genetic rescue was implemented by releasing wild female pumas from Texas into South Florida without knowing whether there were important adaptive differences between the two populations. Identifying adaptive variation specific to Florida panthers may be important to preserving local variation. Almost thirty years after the translocations in 1995, our genetic analysis of 31 PTFPs showed that these admixed individuals retain on average 59%-80% Florida ancestry (*SI Appendix*, Table S1). Moreover, we found that no region of the genome in all Florida panthers was completely replaced by Texas ancestry, indicating that local variation has been preserved with no evidence to date of genetic swamping. On the contrary, we found that Florida ancestry has increased over time following the implementation of genetic rescue (Fig. 6 B and C). A similar observation was made by Onorato et al. (16). One of the objectives of the original plan for genetic rescue was to achieve a level of 20% admixture (12). However, multiple studies have documented levels of admixture above 50% following translocation (13, 16), and we observe a strong subsequent decline in Texas ancestry (Fig. 6 B-D).

The decline in Texas ancestry could be driven by several factors. First, while Texas ancestry may have been initially favored in the Florida population to reduce homozygosity of recessive deleterious variants, it may have brought in novel recessive deleterious variants. Over time, homozygosity for Texas ancestry could have reduced fitness due to homozygosity for these deleterious variants. Importantly, the Texas population likely carried more recessive deleterious variants in the heterozygous state than the prerescue Florida population due to larger population size and higher heterozygosity in the former. Thus, homozygosity for Texas ancestry is predicted to result in more inbreeding depression than homozygosity for FL ancestry (41). Second, it is possible that there are locally adapted alleles in the original Florida ancestry that were not present in the translocated Texas pumas. Consequently, Texas ancestry would not have been favored in Florida and was selected

against. Additionally, cryptic biases in the sampling of panthers over time could be driving this apparent change in ancestry proportions. A final explanation has to do with declining breeding success of the translocated Texas females in Florida. Only five of the eight Texas females were documented to have produced litters and there may have been a tendency of declining reproductive success of these females through time. **Four of the Texas pumas died within 5 y of their release in 1995, reducing the probability of additional admixture.** We note that a multitude of studies have documented the benefits of genetic rescue to this population (13, 14, 16, 42) regardless of the level of admixture and we urge caution in not overinterpreting these changes in ancestry over time. **Continued study of the Florida panthers and sequencing of generations postgenetic rescue could help determine whether these proportions might change in the future.**

We did not find evidence of systematic replacement of ancestry in coding regions. Our results indicate that the proportion of Florida or Texas ancestry is not correlated with gene density. Additionally, we did not find a significant difference in the number of deleterious alleles in Texas and Florida panthers prior to genetic rescue. Both populations had similar levels of deleterious genetic variation (*SI Appendix*, Fig. S3 A, D, and G), however, Florida panthers had substantially higher homozygosity. While these results seem to indicate no ongoing selection for ancestry genome-wide in coding regions, we cannot dismiss the possibility that there are particular regions of the genome where selection has favored Texas or Florida ancestry. However, since the translocation is so recent, detecting specific loci under selection is challenging due to linkage disequilibrium not being broken apart in such few generations (43).

We found no differences in the total number of deleterious alleles per individual in Florida panthers before and after genetic rescue. Instead, a reduction in homozygosity seems to be driving improvements in fitness by reducing the recessive deleterious load. Our results show that PTFPs have much higher heterozygosity and fewer ROHs than CFPs. Our simulations also support these findings, predicting a marked impact of genetic rescue in the presence of recessive variants, but very little impact when only additive variants are present. Finally, simulations predicted that while the genetic rescue was extremely effective at increasing heterozygosity and reducing ROHs, fitness will continue to decrease over the long-term if the population remains small and isolated from conspecifics. This implies that the population will require continued management to remain viable, a supposition that has also been identified in recent population viability models of Florida panthers (14).

Our simulations show that even one single pulse of gene flow (translocations) can have long lasting effects on the heterozygosity (100 generations) (Fig. 4E and *SI Appendix*, Fig. S1). However, this finding is sensitive to many parameters, including N_e and reproductive success, and is probably an optimistic scenario. After 500 generations, in all simulation scenarios, a population of 50 individuals will inevitably suffer an almost complete loss of heterozygosity across the genome and low fitness. These results indicate that a larger population size would be required to maintain heterozygosity and high fitness of the population for extended periods of time. Alternatively, additional translocations for the purpose of genetic rescue could be performed to increase these quantities, although such an approach also has the potential to introduce new deleterious variants. Further analyses are needed to investigate how future genetic rescue attempts would benefit the population.

Our findings agree with previous research on the positive effects of translocation in Florida panthers, resulting in genetic rescue (7, 13–16). However, our genetic load analysis and simulations find that many of these effects might be transient, only temporarily increasing fitness, and that continued management of the Florida

panther will be key to population persistence and recovery. Our simulations show that the translocation on average is beneficial under a wide range of demographic assumptions. However, the long-term benefits of translocations (i.e., >50 generations) on fitness are highly stochastic (*SI Appendix*, Fig. S4). Furthermore, even though translocation is beneficial under the scenarios we have studied, in some cases, such a management initiative may not lead to increased fitness as the specific effects depend on the random distribution of deleterious variants in the genome. These results highlight the inherent uncertainty in the long-term success of translocations. In other species and populations of conservation concern where translocations are being considered, we recommend studies of the deleterious load in both donor and recipient populations before genetic rescue is initiated.

Materials and Methods

Collection of Samples. Field methods used to capture Florida panthers and collect biomedical samples—including blood, tissue and hair for DNA samples—are described in van de Kerk et al. (14). Most of the PTFP samples in this study (26/31) were uncollared individual mortalities and are labeled as (UCFP). A majority of the UCFP samples were roadkills reported by the general public (see *Dataset S1* for more sample details).

DNA, Library Preparation, and Sequencing. We extracted high molecular weight DNA from 29 *P. concolor* individuals. We then sonicated the purified DNA using a Q800R3 Sonicator (QSonica). We sonicated DNA samples for nine minutes total ON time, with a pulse of 15 s ON/15 s OFF, 40% amplitude. Tubes were spun down in a centrifuge every three minutes and then restarted. The target fragment size was ~300 to 500 bp, and we verified this by running 1 μL in a ~1% agarose gel. Sonication was followed by double-sized size selection using lab-made SPRI beads [20% PEG-8000/2.5 M NaCl/1 mg/mL Sera-Mag SpeedBead Carboxylate-Modified Magnetic Particles (Hydrophobic) 65152105050250 (44)] to refine the fragment sizing. These magnetic beads reversibly bind to larger or smaller-sized DNA fragments depending on the volume added. The target size for our libraries was ~350 bp, so we used a 0.5× ratio for the right-side selection and 0.65× for the left-side. We used the Rainin Benchsmart 96, a high-throughput pipetting system to treat samples simultaneously. Then, we used a Kapa HyperPrep library prep kit (Roche Co.) for end repair and A-tailing, followed by adapter ligation with a universal stub. The next step was a postligation bead clean-up to remove excess adapters and ligase. Finally, we performed a 0.8× SPRI cleaning on the Benchsmart.

We performed an indexing PCR with eight cycles. We used a plate provided by the Berkeley Genome Sequencing Facility that contained a premixed unique P5 and P7 indexing oligo for each sample. The Benchsmart was again used to perform a final 0.8× bead clean-up to remove excess indexing oligos and dimers. The target size of fragments after adapter and index is ~450 to 650 bp. After completing the libraries, we performed quality control by measuring the final concentration using a plate reader and Bioanalyzer DNA 1,000 chips to obtain library sizing information. The libraries ranged between 417 and 480 bp, with an adapter of 135 bp, meaning our inserts were ~280 to 345 bp. We sequenced all libraries on one lane of Illumina NovaSeq 6000 150PE Flow Cell S4.

Read Cleaning and Mapping. We used Trimmomatic-0.39 to remove adapters (ILLUMINACLIP:TruSeq3-PE.fa:2:30:10), trim leading and trailing low quality or N bases (below quality 3) (LEADING:3, TRAILING:3) or when the average quality per base drops below 15 in a 4-base sliding window (SLIDINGWINDOW:4:15), and drop reads <75 bp in length (MINLEN:75). All reads were mapped to the *P. yagouaroundi* reference genome GCF_014898765.1 (45)(NCBI Accession No. PRJNA717316), which is an outgroup, using bwa mem. We intentionally used an outgroup as the reference to ensure all populations are equally diverged from the reference. This also allows us to interpret the alleles that match to the reference as ancestral and the nonreference as derived. The mapped alignment files were viewed with the command “samtools view -Sb -F 1804,” followed by sorting and indexing. The binary filter flag -F 1804 excludes unmapped reads (0 × 4), mate unmapped (0 × 8), not primary alignment (0 × 100), reads that fail platform/vendor quality checks (0 × 200) and reads that are PCR or optical duplicate (0 ×

400). We applied these methods to the data that we generated as well as to the publicly available reads we downloaded from Saremi et al. (8) and Ochoa et al. (7). We analyzed 50 individuals in total (Dataset S1), 29 are unique to this study.

Variant Calling and SNP Filtering. We used GATK 4.2 (46) HaplotypeCaller to produce gVCF files for the 50 individuals using the options -ERC BP_RESOLUTION, minimum mapping quality set to 30 and minimum base quality score set to 25. We then generated joint VCF files by passing all individual gVCF files to GATK GenotypeGVCFs using the options -allSites and -stand_call_conf 0. We left aligned and trimmed variants (LeftAlignTrim). We then used a custom filtering script to keep invariant sites and biallelic SNPs. We excluded genotypes with insufficient or excess read depth ($<1/3 \times$ or $>2 \times$ mean read depth for that individual). We excluded sites that did not pass our filtering criteria ($QD < 4$, $FS > 60$, $MQ < 40$, $MQRankSum < -12.5$, $ReadPosRankSum < -8$, $SOR > 3$), with excess missingness ($>25\%$) or excess heterozygosity ($>75\%$). We excluded repeat regions masked by NCBI (identified by Window Masker and additionally masked repetitive sequences identified with RepeatMasker).

Scaffolds that were putatively derived from sex chromosomes or mitochondria were excluded using Plink (v1.90b6.26) (47). For sex chromosomes, we picked 5 PTFP males and 5 PTFP females and plotted the normalized read coverage along the scaffolds using windows (bedtools makewindows -w 100000 -s 10000). When 80% of the windows on a scaffold have an "abnormal" ratio (i.e., male/female coverage >1.15 or <0.85), the scaffold was defined as sex-chromosome-related scaffold. All SNPs from the sex-related scaffolds or windows with abnormal coverage ratio were removed. For mitochondria, scaffold NC_028311.1 was excluded.

Variant Annotation. We used the *P.yagouaroundi* genome and its RefSeq annotation to predict the effects of variants and annotate our vcf files. We used SIFT, a homology-based method, to determine whether an amino acid substitution is deleterious or tolerated (38). To identify LOF variants we used SnpEff (39, 40). We normalized counts (C) within each individual dividing by the total number of sites that pass all the filters in each individual (i). This helps account for different numbers of variants due to differences in coverage. We scaled all of the normalized counts by multiplying by the mean number of sites that pass all the filters (μ_i). The derived allele was defined as the allele that does not match the jaguarundi reference genome (derived = 1, ancestral = 0), as the reference is equidistant to all ingroup puma samples. To count total number of derived alleles (a) per individual in each category we used the formula:

$$a = \left(\frac{C_{0/1}}{i} + 2 \left(\frac{C_{1/1}}{i} \right) \right) * \mu_i,$$

where $C_{0/1}$ is the count of heterozygous genotypes and $C_{1/1}$ is the count of homozygous derived genotypes. To count derived homozygous genotypes (hom) we used the following formula:

$$hom = \left(\frac{C_{1/1}}{i} \right) * \mu_i.$$

Population Structure. We used plink (v1.90b6.26) to apply a minor allele frequency filter (--maf 0.05). Additionally, all variants with one or more multi-character allele codes (--snps-only) or all variants where at least two alternative alleles are present in the dataset (--biallelic-only) were excluded. All variants with missing call rates exceeding 0.5 were excluded (--geno 0.5). We generated the PCA using these sites using plink's pca command (--pca).

We used angsd (48) to generate a beagle file with the same sites and generate genotype likelihoods. The beagle file was converted to lgm format using ped2lgm before feeding into qpas, ancestry component command from OHANA (31). Qpas was run with k = 3, 4. The ancestry component plot was generated using pong (49).

Local Ancestry inference. The chromosome painting was performed using ancestryHMM (33) software and genotype calls. To prepare the data for chromosome painting, the filtered sites were pruned to remove variants in linkage disequilibrium (LD). Variants were removed using plink --indep-pairwise "10 kb 1.16," by setting the window size to be 10 kb, the step size to be 1 variant count, and R^2 threshold to 0.16. Using the python script vcf2ahmm.py (https://github.com/russcd/Ancestry_HMM/scripts), the sites were further filtered by setting the

minimum number of samples in each ancestral population to consider a site to 4 (--min_total 4) and the minimum allele frequency difference between any pair of ancestral populations to include a site to 0.2 (--min_diff 0.2). A total of 284,228 variants passed all filters and were used as input for ancestryHMM. We ran ancestryHMM with the following setting: the overall ancestry proportion of PTFPs was set to be 80% Florida as the indigenous ancestry and 20% Texas, and the admixture time was set five generations ago. These parameter settings were inspired by the OHANA results. The error rate per site was estimated to be 0.01. For each individual, we only kept the sites that had one of the states (0/0, 0/1, 1/1), with a posterior probability $>95\%$. We grouped adjacent SNPs with same ancestry to create intervals; all the positions between the two adjacent SNPs (with no call of ancestry) were assumed to share the same ancestry as their flanking SNPs. These intervals of ancestry were used to compare heterozygosity and ancestry.

Heterozygosity, ROHs, and Relatedness. We calculated the heterozygosity as the proportion of all called genotypes within a single individual that are heterozygous (different between each pair of homologous chromosomes). We used sliding windows across the genome (size = 100 kb, step = 10 kb). Within each window, we calculated the heterozygosity by dividing the count of heterozygotes sites by the total number of called sites.

We calculated relatedness using ngsRelate (32), which uses genotype likelihoods and accounts for inbreeding within a population. We used option -e 0.01 and a minor allele frequency filter of 5%. We identified ROHs with Bcftools (50) roh with option -G 30. To calculate the fraction of the genome in ROH (FROH), we divided the total number of base pairs in ROHs larger than 1 Mb, by the total length of the genome.

Simulations. We simulated the following scenarios: A) Introduction of pumas from TX (translocation) to Florida, and B) the same demographic model as A without translocation. We scaled the parameters by multiplying all population sizes and divergence times by a factor m from the $\Delta\alpha\beta$ model (36) inferred for CFP and TX. Here, m is the ratio of the mutation rate used in that study and the mutation rate (0.5×10^{-8}) that we use in this study based on Saremi et al. (8). For simulating the translocation, we used one single pulse of admixture with exactly five individuals from TX based on the number of Texas pumas that produced offspring (12, 13). For the population sizes of Florida during the severe bottleneck ($N_{FL2} = 7$) and after the population expansion ($N_{FL3} = 50$), we used estimates of the FL census (13) divided by four (51). We considered additional scenarios to account for the uncertainty in the ancestral parameters (SI Appendix, Table S2). Wright-Fisher simulations were conducted using SLiM v4.0.1 (34). We assumed a mutation rate of 0.5×10^{-8} per site per generation and a constant recombination rate of 1×10^{-8} per base pair per generation. We simulated 50 Mbp in each replicate, assuming 10%/90% coding regions and noncoding regions, respectively. We assumed that all mutations accumulating in coding regions were deleterious with a gamma-distributed distribution of fitness effect (DFE) with mean -0.043 and shape parameter $\alpha = 0.23$, estimated by Eyre-Walker et al. (52). We evaluated two dominance effects models: one assuming additive deleterious mutations ($h = 0.5$), and one assuming partially recessive dominance effects determined by the severity of deleterious mutations, where h determined by s [$(h = 0.45, s > -0.001)$, $(h = 0.2, -0.001 \geq s > -0.01)$, $(h = 0.05, -0.01 \geq s > -0.1)$, $(h = 0.0, s \leq -0.1)$ (37)]. Mutations accumulating on noncoding regions were assumed to be neutral ($s = 0$). We assumed log additive interactions among loci under selection, individual fitness (f) in simulations could be calculated by

$$f = \prod_{i \in \text{heterozygous sites}} (1 + h_i s_i) \prod_{j \in \text{homozygous sites}} (1 + s_j).$$

At the beginning of the simulation, all individuals have fitness value 1.0. As variants accumulate over time, the individual fitness changes based on the variants in the genome and their selection coefficients (s) and dominance coefficients (h). Recalculation of individual fitness for each individual is done in each generation of the simulation with the formula provided above, and an average of individual fitness from the donor and recipient populations are recorded throughout simulations. As each simulation contained a 50 Mb of the genome, we aggregated five replicates together by summing the log of the

fitnesses across replicates. This resulted in the simulation of ~25 Mb coding region, approximately the size of a mammalian exome. We then generated 20 replicates for each scenario (*SI Appendix, Fig. S4*) and averaged these together for the results shown in Fig. 5.

To illustrate how genetic rescue affects the heterozygosity of the population, for each model, we randomly selected 20 diploid sampled individuals and output them in a vcf. We calculated the heterozygosity in 100 Kb windows, step 10 Kb using the same custom scripts that were used to calculate heterozygosity for the real data. We concatenated these 20 simulations spatially for each to represent a 50 Mb chromosome.

Gene Density. We used the RefSeq annotation of the *P. yagouaroundi* (NCBI Accession No. PRJNA717316). We extracted all the gene coordinates, by using a command line where the third column of the gff equaled "gene." We used bedtools (53) to generate nonoverlapping windows of 5 Mb along the genome (-makewindows). We kept 5 Mb windows, discarding the fragments at the end of each scaffold that did not complete window length. Then, we used bedtools coverage to count the proportion of each window covered by gene annotations. Finally, we used bedtools intersect to include all of the SNPs analyzed with ancestryHMM that fell within each 5 Mb window. The ancestry of each SNP was calculated by counting all of the alleles of PTFP individuals from Florida and dividing by the total number of alleles with an ancestry assigned at each site. Ancestry was only assigned when the posterior probability was higher than 95%. Using dplyr library (54) and custom scripts in R, we averaged their ancestry to obtain a mean value of ancestry proportion per window. We compared the gene density and the ancestry proportion, and fitted a linear regression to test for a correlation.

Selection Scans. We used *angsd* (49) to perform selection scans using genotype likelihoods. First, we calculated the SFS and the 2d-SFS using *angsd -doSaf*, followed by *realSFS*. We performed a scan of F_{ST} in 100 Kb windows with 20 Kb steps (*realSFS fst stats2 pop1.pop2.fst.idx -win 100000 -step 20000 -type 2*) with the following combinations 1) CFPs – TX, 2) PTFPs – TX, and 3) PTFPs – CFPs. We used thetaStat do _stat to calculate Tajima's D and average number of pairwise differences (tp) within each population (TX, CFP, and PTFP) in 100 Kb windows with 20 Kb steps.

Disclaimers

Any use of trade, firm, or product names is for descriptive purposes only and does not imply endorsement by the U.S. Government.

Although this code has been processed successfully on a computer system at the University of California, no warranty expressed or implied is made regarding the display or utility of the data for other purposes, nor on all computer systems, nor shall the act of distribution constitute any such warranty. The USGS or the U.S. Government shall not be held liable for improper or incorrect use of the data described and/or contained herein.

Data, Materials, and Software Availability. Reads and code data have been deposited in SRA ([PRJNA898112](#)) (29) and GitHub (<https://github.com/aguilar-gomez/pumaRescue>) (35), respectively.

ACKNOWLEDGMENTS. D.A.-G. was supported by a Chancellor's Postdoctoral Fellowship from the University of California, Los Angeles. K.E.L. was supported by the NIH Grant R35GM119856. Florida panther samples were collected using funding from the Florida Panther Research and Management Trust Fund.

Author affiliations: ^aDepartment of Ecology and Evolutionary Biology, University of California, Los Angeles, CA 90095; ^bCenter for Computational Biology, College of Computing, Data Science and Society, University of California, Berkeley, CA 94720; ^cCell and Molecular Biology Programme, School of Life Sciences, The Chinese University of Hong Kong, Hong Kong, Special Administrative Region of China; ^dDepartment of Ecology & Evolutionary Biology, Yale University, New Haven, CT 06520; ^eU.S. Geological Survey, Arizona Cooperative Fish and Wildlife Research Unit, University of Arizona, Tucson, AZ 85721; ^fSchool of Natural Resources and the Environment, University of Arizona, Tucson, AZ 85721; ^gDepartment of Biology, Genomics and Bioinformatics Cluster, University of Central Florida, Orlando, FL 32816; ^hFish and Wildlife Research Institute, Florida Fish and Wildlife Conservation Commission, Naples, FL 34114; and ⁱDepartment of Human Genetics, David Geffen School of Medicine, University of California, Los Angeles, CA 90095

Author contributions: D.A.-G., Y.Z., K.E.L., and R.N. designed research; D.A.-G., L.Y., and Y.Z. performed research; D.A.-G. and L.Y. analyzed data; A.O., M.C., and R.R.F. helped contextualize the results; D.O. provided the samples and helped to contextualize the results; and D.A.-G., A.O., D.O., K.E.L., and R.N. wrote the paper.

1. M. Sunquist, F. Sunquist, *Wild Cats of the World* (University of Chicago Press, 2002).
2. D. Onorato *et al.*, "Long-term research on the Florida panther (*Puma concolor coryi*): Historical findings and future obstacles to population persistence" in *Biology and Conservation of Wild Felids*, D.W. MacDonald, A.J. Loveridge, Eds. (Oxford University Press, 2010), pp. 453–469.
3. R. T. McBride, R. T. McBride, R. M. McBride, C. E. McBride, Counting pumas by categorizing physical evidence. *Southeast. Nat.* **7**, 381–400 (2008).
4. S. J. O'Brien, Genetic introgression within the Florida panther *Felis concolor coryi*. *Natl. Geogr. Res.* **6**, 485 (1990).
5. M. E. Roelke, J. S. Martenson, S. J. O'Brien, The consequences of demographic reduction and genetic depletion in the endangered Florida panther. *Curr. Biol.* **3**, 340–350 (1993).
6. M. Culver, W. E. Johnson, J. Pecon-Slattery, S. J. O'Brien, Genomic ancestry of the American puma (*Puma concolor*). *J. Hered.* **91**, 186–197 (2000).
7. A. Ochoa, D. P. Onorato, R. R. Fitak, M. E. Roelke-Parker, M. Culver, De novo assembly and annotation from parental and F1 Puma genomes of the Florida Panther Genetic Restoration Program. *G3* **9**, 3531–3536 (2019).
8. N. F. Saremi *et al.*, Puma genomes from North and South America provide insights into the genomic consequences of inbreeding. *Nat. Commun.* **10**, 4769 (2019).
9. G. K. Zimmer, Animal release in Everglades National Park. *National Park Magazine* **10** (1966).
10. M. E. Roelke *et al.*, Seroprevalence of infectious disease agents in free-ranging Florida panthers (*Felis concolor coryi*). *J. Wildl. Dis.* **29**, 36–49 (1993).
11. U. S. Seal, R. C. Lacy, J. D. Ballou, T. J. Foose, Florida panther population viability analysis (Report to US Fish and Wildlife Service, Captive Breeding Specialist Group, Apple Valley, MN, 1989).
12. U. S. Seal, "A plan for genetic restoration and management of the Florida panther (*Felis concolor coryi*)" (Report to the Florida Game and Fresh Water Fish Commission, Conservation Breeding Specialist Group, Rep. 1, Apple Valley, MN (1994)).
13. W. E. Johnson *et al.*, Genetic restoration of the Florida panther. *Science* **329**, 1641–1645 (2010).
14. M. Kerk, D. P. Onorato, J. A. Hostetler, B. M. Bolker, M. K. Oli, Dynamics, persistence, and genetic management of the endangered Florida panther population. *Wildl. Monogr.* **203**, 3–35 (2019).
15. A. Ochoa, D. P. Onorato, M. E. Roelke-Parker, M. Culver, R. R. Fitak, Give and take: Effects of genetic admixture on mutation load in endangered Florida panthers. *J. Hered.* **113**, 491–499 (2022).
16. D. P. Onorato *et al.*, Multi-generational benefits of genetic rescue. *Sci. Rep.* **14**, 17519 (2024).
17. Florida Fish and Wildlife Conservation Commission, Annual report on the research and management of Florida panthers: 2022–2023 (Fish and Wildlife Research Institute & Division of Habitat and Species Conservation, Naples, FL, 2023).
18. K. Ralls, P. Sunnucks, R. C. Lacy, R. Frankham, Genetic rescue: A critique of the evidence supports maximizing genetic diversity rather than minimizing the introduction of putatively harmful genetic variation. *Biol. Conserv.* **251**, 108784 (2020).
19. J. A. Robinson *et al.*, Genomic signatures of extensive inbreeding in Isle Royale wolves, a population on the threshold of extinction. *Sci. Adv.* **5**, eaau0757 (2019).
20. J. A. Robinson, C. Brown, B. Y. Kim, K. E. Lohmueller, R. K. Wayne, Purging of strongly deleterious mutations explains long-term persistence and absence of inbreeding depression in island foxes. *Curr. Biol.* **28**, 3487–3494.e4 (2018).
21. P. W. Hedrick, A. Garcia-Dorado, Understanding inbreeding depression, purging, and genetic rescue. *Trends Ecol. Evol.* **31**, 940–952 (2016).
22. J. Robinson, C. C. Kyriazis, S. C. Yuan, K. E. Lohmueller, Deleterious variation in natural populations and implications for conservation genetics. *Annu. Rev. Anim. Biosci.* **11**, 93–114 (2023).
23. Y. Zhang, A. J. Stern, R. Nielsen, The evolutionary dynamics of local adaptations under genetic rescue is determined by mutational load and polygenicity. *J. Hered.* **115**, 373–384 (2023), 10.1093/jhered/esad079.
24. K. Harris, Y. Zhang, R. Nielsen, Genetic rescue and the maintenance of native ancestry. *Conserv. Genet.* **20**, 59–64 (2019).
25. S. W. Fitzpatrick *et al.*, Genomic and fitness consequences of genetic rescue in wild populations. *Curr. Biol.* **30**, 517–522.e5 (2020).
26. J. R. Adams, L. M. Vucetich, P. W. Hedrick, R. O. Peterson, J. A. Vucetich, Genomic sweep and potential genetic rescue during limiting environmental conditions in an isolated wolf population. *Proc. Biol. Sci.* **278**, 3336–3344 (2011).
27. B. Y. Kim, C. D. Huber, K. E. Lohmueller, Deleterious variation shapes the genomic landscape of introgression. *PLoS Genet.* **14**, e1007741 (2018).
28. A. S. Hwang, S. L. Northrup, D. L. Peterson, Y. Kim, S. Edmonds, Long-term experimental hybrid swarms between nearly incompatible *Tigriopus californicus* populations: Persistent fitness problems and assimilation by the superior population. *Conserv. Genet.* **13**, 567–579 (2012).
29. D. Aguilar-Gómez, Post-translocation Florida Panthers: Big Cypress X Texas. Sequence Read Archive. <https://www.ncbi.nlm.nih.gov/bioproject/PRJNA898112>. Deposited 4 November 2022.
30. USFWS, *Species Status Assessment for the Florida Panther* (U.S. Fish & Wildlife Service, 2020).
31. J. Y. Cheng, T. Mailund, R. Nielsen, Fast admixture analysis and population tree estimation for SNP and NGS data. *Bioinformatics* **33**, 2148–2155 (2017).
32. K. Hangjai, I. Moltke, P. A. Andersen, A. Manica, T. S. Korneliussen, Fast and accurate relatedness estimation from high-throughput sequencing data in the presence of inbreeding. *Gigascience* **8**, giz034 (2019).
33. R. Corbett-Detig, R. Nielsen, A hidden Markov model approach for simultaneously estimating local ancestry and admixture time using next generation sequence data in samples of arbitrary ploidy. *PLoS Genet.* **13**, e1006529 (2017).
34. B. C. Haller, P. W. Messer, SLiM 4: Multispecies eco-evolutionary modeling. *Am. Nat.* **201**, E127–E139 (2023).
35. D. Aguilar-Gómez, Y. Zhang, L. Yuan, pumaRescue [Computer software]. GitHub. <https://github.com/aguilar-gomez/pumaRescue/>. Deposited 16 January 2024.

36. P. D. Blischak, M. S. Barker, R. N. Gutenkunst, Inferring the demographic history of inbred species from genome-wide SNP frequency data. *Mol. Biol. Evol.* **37**, 2124–2136 (2020).
37. C. C. Kyriazis, J. A. Robinson, K. E. Lohmueller, Using computational simulations to model deleterious variation and genetic load in natural populations. *Am. Nat.* **202**, 737–752 (2023).
38. P. C. Ng, S. Henikoff, SIFT: Predicting amino acid changes that affect protein function. *Nucleic Acids Res.* **31**, 3812–3814 (2003).
39. P. Cingolani, Variant annotation and functional prediction: SnpEff. *Methods Mol. Biol.* **2493**, 289–314 (2022).
40. P. Cingolani *et al.*, A program for annotating and predicting the effects of single nucleotide polymorphisms, SnpEff: SNPs in the genome of *Drosophila melanogaster* strain w1118; iso-2; iso-3. *Fly* **6**, 80–92 (2012).
41. C. C. Kyriazis, R. K. Wayne, K. E. Lohmueller, Strongly deleterious mutations are a primary determinant of extinction risk due to inbreeding depression. *Evol. Lett.* **5**, 33–47 (2021).
42. J. A. Hostetler *et al.*, Genetic introgression and the survival of Florida Panther kittens. *Biol. Conserv.* **143**, 2789–2796 (2010).
43. J. E. Crawford, R. Nielsen, Detecting adaptive trait loci in nonmodel systems: Divergence or admixture mapping? *Mol. Ecol.* **22**, 6131–6148 (2013).
44. P. Jolivet, J. W. Foley, SPRI bead mix v1. ZappyLab, Inc. <https://doi.org/10.17504/protocols.io.bnz4mf8w>. Deposited 26 October 2020.
45. G. Tamazian *et al.*, Draft de novo genome assembly of the elusive jaguarundi, *Puma yagouaroundi*. *J. Hered.* **112**, 540–548 (2021).
46. G. A. Van der Auwera, B. D. O'Connor, *Genomics in the Cloud: Using Docker, GATK, and WDL in Terra* (O'Reilly Media, Inc., 2020).
47. S. Purcell, C. Chang, PLINK2 (v1. 90b6. 9). <https://www.cog-genomics.org/plink/2.0>. Accessed 10 November 2023.
48. T. S. Korneliussen, A. Albrechtsen, R. Nielsen, ANGSD: Analysis of next generation sequencing data. *BMC Bioinf.* **15**, 356 (2014).
49. A. A. Behr, K. Z. Liu, G. Liu-Fang, P. Nakka, S. Ramachandran, pong: Fast analysis and visualization of latent clusters in population genetic data. *Bioinformatics* **32**, 2817–2823 (2016).
50. P. Danecek *et al.*, Twelve years of SAMtools and BCFtools. *Gigascience* **10**, giab008 (2021).
51. F. P. Palstra, D. J. Fraser, Effective/census population size ratio estimation: A compendium and appraisal. *Ecol. Evol.* **2**, 2357–2365 (2012).
52. A. Eyre-Walker, M. Woolfit, T. Phelps, The distribution of fitness effects of new deleterious amino acid mutations in humans. *Genetics* **173**, 891–900 (2006).
53. A. R. Quinlan, BEDTools: The Swiss-army tool for genome feature analysis. *Curr. Protoc. Bioinf.* **47**, 11–12 (2014).
54. H. Wickham, R. François, L. Henry, K. Müller, D. Vaughan, dplyr: A grammar of data manipulation (2023). <https://dplyr.tidyverse.org>. Accessed 1 July 2023.

Supplementary Information for Genetic rescue of Florida panthers reduced homozygosity but did not swamp ancestral genotypes

Diana Aguilar-Gómez^{a,b,*}, Lin Yuan^c, Yulin Zhang^b, Alexander Ochoa^d, Melanie Culver^{e,f}, Robert R. Fitak^g, Dave Onorato^h, Kirk E. Lohmueller^{a,*}, and Rasmus Nielsen^{b,*}

^aDepartment of Ecology and Evolutionary Biology, University of California, Los Angeles, CA 90095

^bCenter for Computational Biology, College of Computing, Data Science and Society, University of California, Berkeley, CA 94720

^cCell and Molecular Biology Programme, School of Life Sciences, The Chinese University of Hong Kong, New Territories, Hong Kong Special Administrative Region of China

^dDepartment of Ecology & Evolutionary Biology, Yale University, New Haven, CT 06520

^eU.S. Geological Survey, Arizona Cooperative Fish and Wildlife Research Unit, University of Arizona, Tucson, AZ 85721

^fSchool of Natural Resources and the Environment, University of Arizona, Tucson, AZ 85721

^gDepartment of Biology, Genomics and Bioinformatics Cluster, University of Central Florida, Orlando, FL 32816

^hFish and Wildlife Research Institute, Florida Fish and Wildlife Conservation Commission, Naples, FL 34114

*corresponding authors: Diana Aguilar-Gómez, Kirk Lohmueller and Rasmus Nielsen

Email: aguilargomez@ucla.edu, rasmus_nielsen@berkeley.edu, klohmueler@ucla.edu

Author Contributions: R.N., K.E.L. and D.A.G designed the research. D.O. provided the samples. D.A.G did the library prep. D.A.G and L.Y. did all the bioinformatic analyses. Y.Z. performed the simulations. D.A.G, R.N., K.E.L., D.O. and A.O. wrote the paper. All authors read, gave feedback and approved the current version of the manuscript.

Competing Interest Statement: No competing interest.

Classification: Biological Sciences, Evolution, Genetics

Keywords: genetic rescue, puma, conservation genomics, genetic swamping

This PDF file includes:

Supplementary Text

Supplementary Figures 1 to 4

Supplementary Tables 1 to 3

Supplementary Text

Ancestry discrepancies

In this study, we combined whole-genome sequence data with population genetic simulations to investigate the genomic impact of genetic rescue in the FL panthers. Some of the PTFP individuals do not appear admixed according to their genome-wide ancestry components as inferred using OHANA (Fig. 1D). In a recent study, it was similarly found that not all pumas post-genetic rescue had TX ancestry (1). However, AncestryHMM estimates all PTFPs to have Texas ancestry. In the two F₁ individuals, OHANA underestimates Texas ancestry to 40% and 44%, respectively, instead of the expected 50%, suggesting that the discrepancy is due to a downward bias in the OHANA analyses. OHANA is an unsupervised method and not even all TX individuals are inferred to have 100% TX ancestry (Fig. 1B), suggesting that the bias might be due to latent shared genetic variation between PTFP and Texas, possibly through gene-flow with a, now extinct, third population. The supervised analysis in ancestryHMM infers the genomes of both F₁s to be more than 91% of the diploid genomic positions FL/TX with 50% contribution from each ancestry. It underestimates the heterozygous sites (FL/TX) but correctly estimates 50% contribution from each parental population. For the local ancestry analysis, having a Central American sample as a third reference panel could result in more accurate estimates and possibly less discrepancies between OHANA and ancestryHMM. However, our results using South American pumas showed that PTFPs do not have a large proportion of this third ancestry.

The Florida Panthers at Everglades

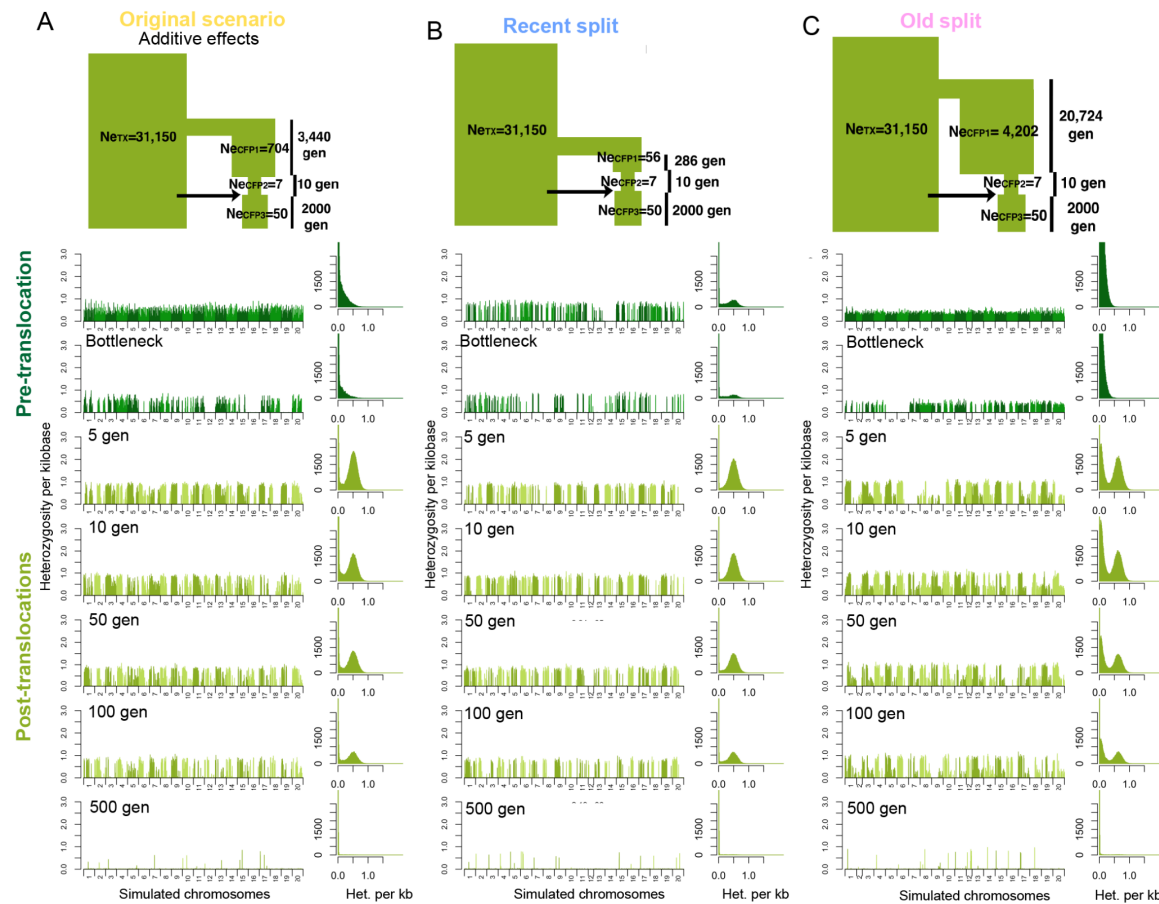
Panthers historically present in Everglades National Park, including those with EVG ancestry (mixed canonical FP and Central American puma), face unique challenges, particularly due to their isolation from the core population of panthers (CFP and PTFP) in southwestern Florida resulting from the semi-permeable barrier associated with fluctuating water levels in Shark River Slough (Figure 1B) (2). Additionally, there is only a small portion of Everglades National Park that is considered quality habitat for panthers as most of Florida's east coast is heavily developed, severely limiting the local carrying capacity. The combination of limited gene flow and small population size in Everglades National Park (2, 3), likely has resulted in high levels of inbreeding in the area and, therefore, a high content of ROHs, as seen in our results and previous studies (4). Our findings of high heterozygosity and a high proportion of long ROHs in EVG can be reconciled by the demographic history including admixture in this region. They also match our simulation predictions, where it is possible to have higher heterozygosity and still present ROHs and lower fitness, although an even more extreme scenario is observed in EVG as it never experienced a population expansion after the bottleneck. Due to these factors, this subpopulation is likely to always be tenuous and even ephemeral (2) even with population management. Florida panthers in Big Cypress (CFP and PTFP) are likely less impacted because they are the main portion of the Florida panther population.

References

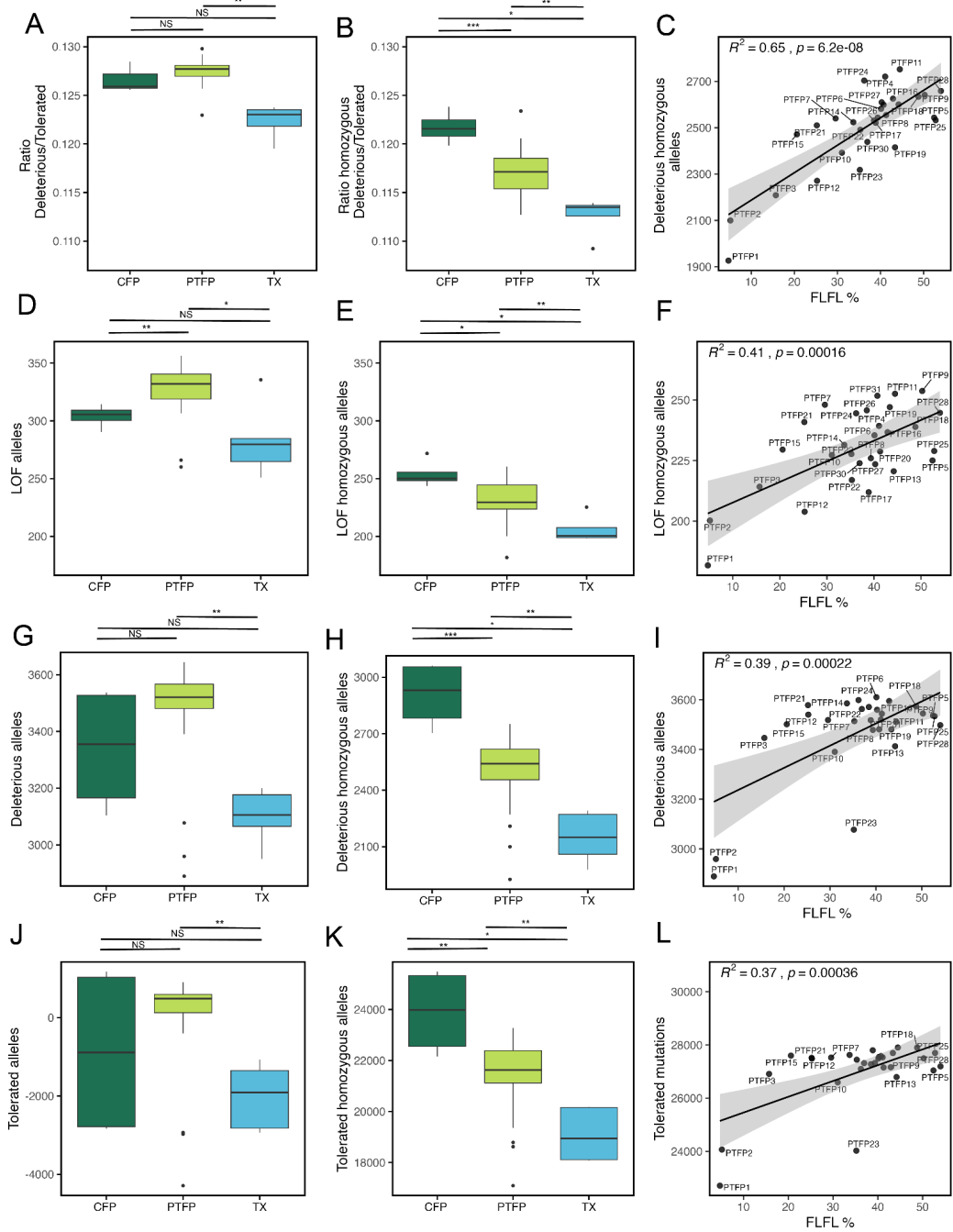
1. L. M. Penfold, *et al.*, Long-term evaluation of male Florida panther (*Puma concolor coryi*) reproductive parameters following genetic introgression. *J. Mammal.* **103**, 835–844 (2022).
2. D. Onorato, *et al.*, Long-term research on the Florida panther (*Puma concolor coryi*): historical findings and future obstacles to population persistence. *Biology and conservation of wild felids* 453–469 (2010).
3. D. P. Onorato, *et al.*, Habitat selection by critically endangered Florida panthers across the diel period: implications for land management and conservation. *Anim. Conserv.* **14**, 196–205 (2011).
4. N. F. Saremi, *et al.*, Puma genomes from North and South America provide insights into the genomic consequences of inbreeding. *Nat. Commun.* **10**, 4769 (2019).
5. P. D. Blischak, M. S. Barker, R. N. Gutenkunst, Inferring the Demographic History of Inbred Species from Genome-Wide SNP Frequency Data. *Mol. Biol. Evol.* **37**, 2124–2136 (2020).

6. A. Ochoa, D. P. Onorato, R. R. Fitak, M. E. Roelke-Parker, M. Culver, De Novo Assembly and Annotation from Parental and F1 Puma Genomes of the Florida Panther Genetic Restoration Program. *G3* **9**, 3531–3536 (2019).

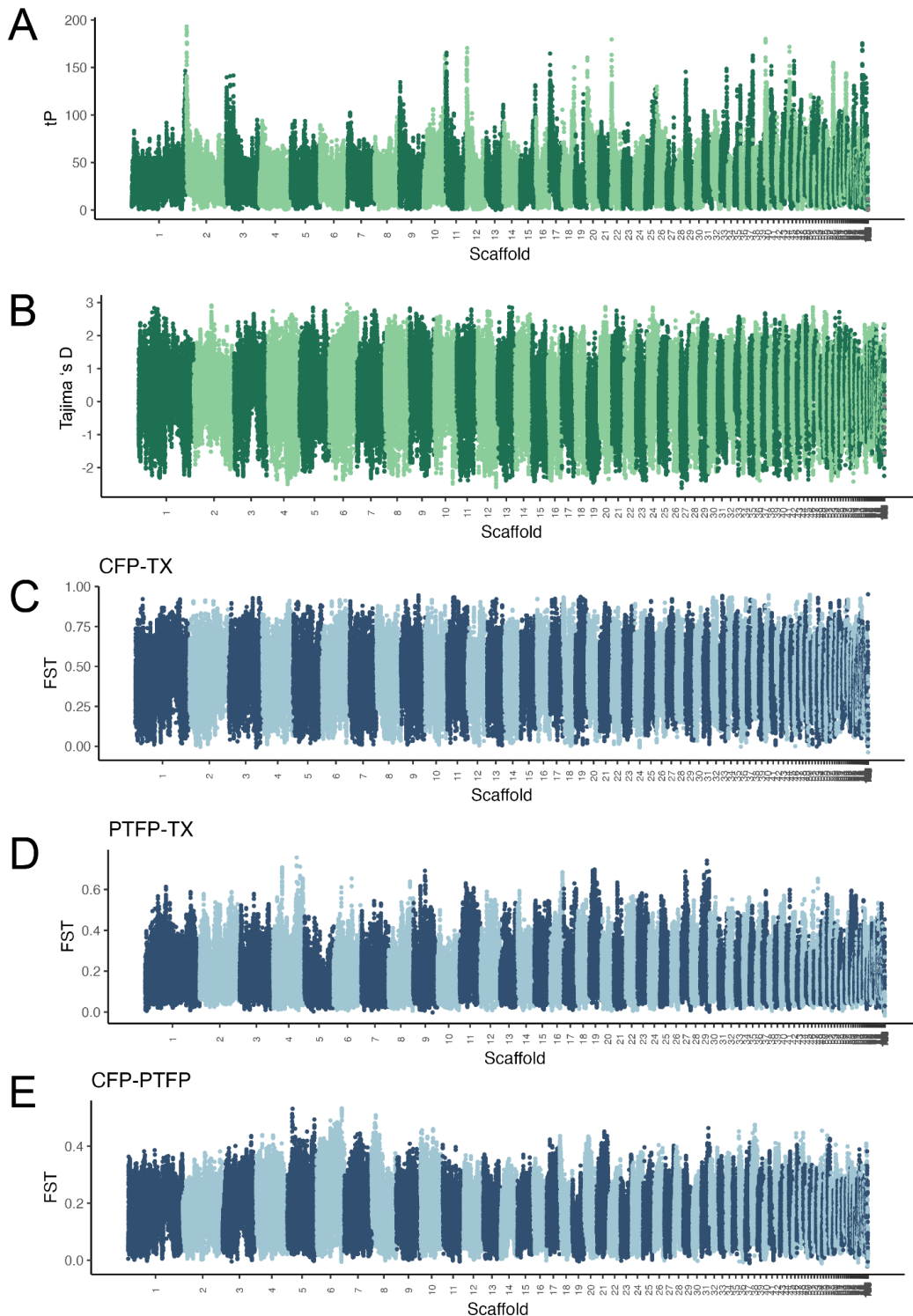
Supplementary Figures and Tables



Supplemental Figure 1. Heterozygosity in additional models. A) Original model with additive dominance effects B) Model with a more recent split time between Texas and Florida populations. C) Model with older split time between Texas and Florida populations. See Supplementary Table 4 for the specific parameter values assumed.

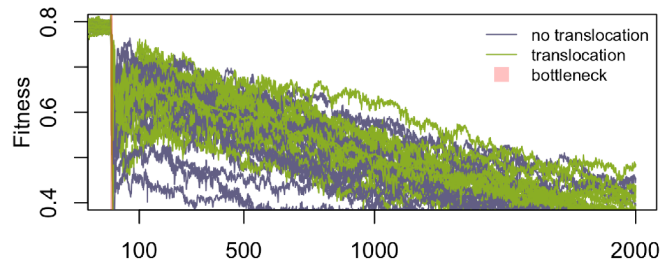
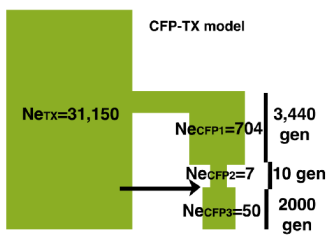


Supplementary Figure 2. Deleterious genetic variation. Boxplots with individuals separated by population Canonical Florida Panther (CFP), Post-translocation Florida Panther (PTFP) and Texas (TX). On top of each boxplot bars with Wilcoxon p-values: * <0.05, ** <0.01, *** <0.001, NS non-significant. A) Ratio of deleterious/tolerated all alleles B) Ratio of deleterious/tolerated homozygous alleles C) Linear regression, using only PTFP individuals: homozygous deleterious alleles ~ proportion of genome with homozygous ancestry from Florida (FLFL%) D) Loss of function (LOF) all alleles, E) LOF homozygous alleles, F) Linear regression, PTFP individuals: LOF homozygous alleles ~ FLFL% G) Deleterious alleles H) Deleterious homozygous allele I) Linear regression, PTFP individuals: deleterious alleles ~ FLFL% J) Tolerated alleles K) Tolerated homozygous allele L) Linear regression, PTFP individuals: tolerated alleles ~ FLFL%.

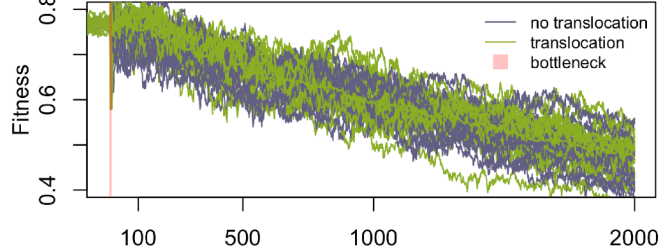
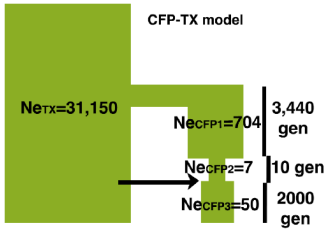


Supplementary Figure 3. Selection scans using 100Kb windows with 20kb steps. A) Average pairwise number of mutations (tP) in PTFP B) Tajima's D in PTFP C) F_{ST} scan between CFP and TX D) F_{ST} scan between PTFP and TX E) F_{ST} scan between CFP and PTFP.

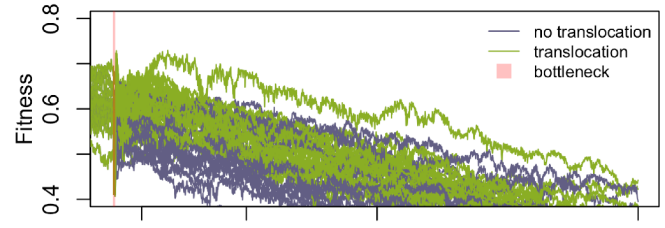
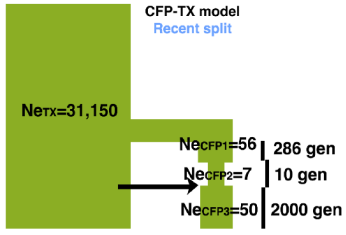
A Partially recessive effects



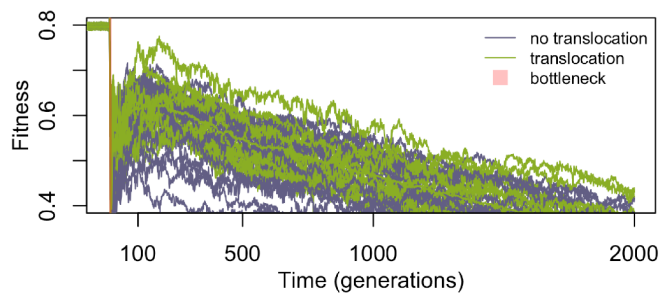
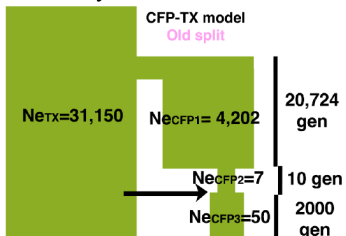
B Additive effects



C Partially recessive effects



D Partially recessive effects



Supplementary Figure 4. Replicates of simulations. Demographic models used are shown on the left plots. Individual simulation replicates (each consisting of ~25Mb of coding sequence) are shown in the plots on the right. A) Partially recessive original model B) Additive effects original model C) Partially recessive recent split model D) Partially recessive old split model.

Supplementary Table 1. Inference of genome-wide ancestry using AncestryHMM and OHANA

Individual	AncestryHMM					OHANA, k=4		Collection date
	FL	TX	FLFL	FLTX	TXTX	Florida	Texas	
PTFP1	50	50	4	91	5	56	44	
PTFP10	56	44	29	54	17	64	36	3/16/2013
PTFP11	59	41	42	35	24	92	8	10/11/2016
PTFP12	53	47	23	60	17	79	9	1/19/2017
PTFP13	64	36	42	44	14	86	14	5/3/2016
PTFP14	53	47	32	43	25	94	6	6/29/2013
PTFP15	48	52	20	56	24	46	54	3/24/2014
PTFP16	64	36	42	45	13	81	19	4/26/2016
PTFP17	63	37	36	54	11	86	14	6/11/2015
PTFP18	67	33	47	41	12	99	1	10/18/2016
PTFP19	62	38	42	41	17	81	15	4/28/2016
PTFP2	50	50	4	92	4	60	40	
PTFP20	59	41	39	38	22	97	3	4/6/2016
PTFP21	47	53	24	47	29	44	56	4/30/2011
PTFP22	56	44	33	45	22	87	13	8/6/2014
PTFP23	56	44	34	45	21	86	14	11/13/2014
PTFP24	57	43	35	45	20	60	40	12/18/2014
PTFP25	71	29	50	40	9	92	6	2/27/2017
PTFP26	59	41	36	47	17	85	15	12/31/2014
PTFP27	58	42	38	41	21	100	0	7/6/2015
PTFP28	71	29	53	37	10	99	1	3/14/2017
PTFP29	76	24	60	33	7	100	0	4/5/2017
PTFP3	38	62	15	47	38	44	56	3/17/2014
PTFP30	59	41	35	48	18	86	9	12/18/2014
PTFP31	59	41	39	42	20	90	10	3/9/2016
PTFP4	60	40	38	44	18	100	0	1/21/2016
PTFP5	71	29	50	43	7	90	0	12/9/2016
PTFP6	63	37	39	48	13	66	34	4/6/2016
PTFP7	57	43	28	57	15	56	44	11/19/2012
PTFP8	60	40	38	45	17	82	17	10/8/2015
PTFP9	68	32	48	40	12	91	9	10/31/2016
mean	59	41	35	48	17	80	19	

Supplementary Table 2. Models tested to account for uncertainty. The original parameters and confidence values are from the $\partial\alpha\bar{\alpha}$ model (5), scaled to the mutation rate (0.5×10^{-8}).

Parameters	Original model	CI 95%		Recent split	Old split
		Lower - upper			
NeTX	31,150	27,852	- 34,848	31,150	31,150
NeCFP1	704	56	- 8,404	56	4,202
NeCFP2	7	NA		7	7
NeCFP3	50	NA		50	50
T _s	3,440	286	- 41,448	286	20,724

Supplementary Table 3. Average fitness of simulations. In this table we show the average fitness value of simulations for the four models tested and the translocation (T) and no translocation (NT) scenarios for each of them. Each column is the average fitness in the simulated canonical Florida panther (CFP) population. The rows represent different timepoints of the simulation. The rows called x generations, represent the number of generations after the bottleneck.

				Partially recessive dominance effects						Additive dominance effects	
				Original		Old split		Recent split			
Before bottleneck	*	Ne	gen	T	NT	T	NT	T	NT	T	NT
		153896	0.786	0.786	0.797	0.797	0.602	0.602	0.768	0.768	
		153897	0.788	0.788	0.797	0.797	0.597	0.597	0.768	0.768	
		153898	0.787	0.787	0.797	0.797	0.597	0.597	0.768	0.768	
		153899	0.788	0.788	0.797	0.797	0.603	0.603	0.768	0.768	
Bottleneck	7	153900	0.788	0.788	0.798	0.798	0.603	0.603	0.767	0.767	
		153901	0.788	0.788	0.797	0.797	0.600	0.600	0.768	0.768	
		153902	0.794	0.794	0.798	0.798	0.601	0.601	0.760	0.760	
		153903	0.736	0.736	0.718	0.718	0.578	0.578	0.756	0.756	
		153904	0.701	0.701	0.639	0.639	0.583	0.583	0.752	0.752	
		153905	0.665	0.665	0.561	0.561	0.572	0.572	0.740	0.740	
		153906	0.641	0.641	0.530	0.530	0.568	0.568	0.743	0.743	
		153907	0.625	0.625	0.518	0.518	0.570	0.570	0.752	0.752	
		153908	0.602	0.602	0.458	0.458	0.560	0.560	0.748	0.748	
		153909	0.577	0.577	0.448	0.448	0.544	0.544	0.744	0.744	
		153910	0.562	0.562	0.393	0.393	0.549	0.549	0.742	0.742	

Translocation	12	153911	0.543	0.543	0.407	0.407	0.552	0.552	0.743	0.743
		153912	0.637	0.528	0.554	0.402	0.648	0.548	0.763	0.739
5 generations	50	153913	0.682	0.528	0.633	0.404	0.679	0.545	0.762	0.736
		153914	0.664	0.543	0.626	0.412	0.679	0.546	0.761	0.739
		153915	0.664	0.544	0.621	0.429	0.663	0.549	0.761	0.736
		153916	0.655	0.557	0.610	0.435	0.656	0.552	0.763	0.739
		153917	0.652	0.560	0.598	0.449	0.644	0.552	0.760	0.740
		153918	0.646	0.574	0.598	0.456	0.645	0.553	0.760	0.741
		153919	0.637	0.574	0.598	0.464	0.638	0.556	0.762	0.741
		153920	0.633	0.575	0.588	0.469	0.633	0.555	0.763	0.741
		153921	0.629	0.577	0.594	0.471	0.623	0.556	0.763	0.745
		153922	0.630	0.584	0.580	0.479	0.629	0.556	0.761	0.748
10 generations	50	153923	0.624	0.589	0.582	0.493	0.616	0.555	0.765	0.748
		153924	0.622	0.588	0.576	0.494	0.599	0.556	0.763	0.748
		153925	0.615	0.595	0.577	0.497	0.606	0.558	0.760	0.746
		153926	0.608	0.592	0.565	0.502	0.605	0.559	0.763	0.750
		153921	0.629	0.577	0.594	0.471	0.623	0.556	0.763	0.745
15 generations	50	153961	0.619	0.628	0.591	0.560	0.605	0.564	0.765	0.738
		154011	0.646	0.627	0.616	0.592	0.614	0.555	0.754	0.738
		154411	0.583	0.553	0.547	0.513	0.544	0.494	0.673	0.665
		154911	0.507	0.467	0.471	0.447	0.465	0.422	0.595	0.604
2000 generations		155910	0.366	0.344	0.330	0.320	0.331	0.300	0.473	0.458